MEASUREMENTS OF REFLECTION AND TRANSMISSION IN A LASER-PRODUCED PLASMA

Thomas Harold Butler

DUDLEY KNOX LIBRARY
NAVAL POSTGRADUATE SCHOOL
MONTEREY CA 93943

NAVAL POSTGRADUATE SCHOOL
Monterey, California

THESIS

MEASUREMENTS OF REFLECTION AND TRANSMISSION

IN A LASER-PRODUCED PLASMA

by

Thomas Harold Butler

December 1974

Thesis Advisor: A. W. Cooper

Approved for public release; distribution unlimited.

T 165275

SECURITY CLASSIFICATION OF THIS PAGE (When Data Entered)

REPORT DOCUMENTATION PAGE		READ INSTRUCTIONS BEFORE COMPLETING FORM
1. REPORT NUMBER	2 GOVT ACCESSION NO.	3. RECIPIENT'S CATALOG NUMBER
4. TITLE (and Subtitle) Measurements of Reflection and Transmission in a Laser-Produced Plasma		5. TYPE OF REPORT & PERIOD COVERED Master's Thesis; December 1974 6. PERFORMING ORG. REPORT NUMBER
7. AUTHOR(s) Thomas Harold Butler		8. CONTRACT OR GRANT NUMBER(s)
9. PERFORMING ORGANIZATION NAME AND ADDRESS Naval Postgraduate School Monterey, California 93940		10. PROGRAM ELEMENT, PROJECT, TASK AREA & WORK UNIT NUMBERS
11. CONTROLLING OFFICE NAME AND ADDRESS Naval Postgraduate School Monterey, California 93940		12. REPORT DATE December 1974 13. NUMBER OF PAGES
14. MONITORING AGENCY NAME & ADDRESS(if different from Controlling Office) Naval Postgraduate School Monterey, California 93940		15. SECURITY CLASS. (of this report) Unclassified 15a. DECLASSIFICATION/DOWNGRADING SCHEDULE

16. DISTRIBUTION STATEMENT (of this Report)

Approved for public release; distribution unlimited

17. DISTRIBUTION STATEMENT (of the abstract entered in Block 20, if different from Report)

18. SUPPLEMENTARY NOTES

19. KEY WORDS (Continue on reverse side if necessary and identify by block number)

20. ABSTRACT (Continue on reverse side if necessary and identify by block number)

A high energy laser with a pulse width of 30 nsecs (FWHM) irradiated an aluminum target at an angle 30^{o} from the target's normal. The power density at the target's surface was varied between 10^{8} and $10^{10} W/cm^{2}$. Measurements were made of the reflective and transmissive characteristics of the ablated surface particles, and from the measured data, an absorption coefficient was inferred. At intensities greater than $10^{9} W/cm^{2}$

DD FORM 1 JAN 73 1473 EDITION OF 1 NOV 65 IS OBSOLETE
S/N 0102-014-6601 |
(Page 1)

SECURITY CLASSIFICATION OF THIS PAGE (When Data Entered)

the transmitted beam showed a cutoff approximately 25 nsecs after the start of the laser pulse, indicative of the formation of an overdense plasma. All reflection measurements showed that the scattering was primarily specular. At intensities between 10^8 and $10^9 W/cm^2$, the reflected beam exhibited a narrow pulse attributable to thermal damage at the target surface. At intensities of $10^9 W/cm^2$ or greater, the reflected beam also indicated a sharp decrease in amplitude attributed to absorption in the newly-formed plasma. The value of the absorption coefficient was calculated to be 0.545.

Measurements of Reflection and Transmission In a Laser-Produced Plasma

by

Thomas Harold Butler
Lieutenant Commander, United States Navy
B.S., Holy Cross College, 1964

Submitted in partial fulfillment of the
requirements for the degree of

MASTER OF SCIENCE IN PHYSICS

from the

NAVAL POSTGRADUATE SCHOOL
December 1974

Thesis
B947
c.1

DUD FI
NAVAL
MONTEREY, CALIFORNIA 93940

ABSTRACT

A high energy laser with a pulse width of 30 nsecs (FWHM) irradiated an aluminum target at an angle 30^{o} from the target's normal. The power density at the target's surface was varied between 10^{8} and $10^{10}W/cm^{2}$. Measurements were made of the reflective and transmissive characteristics of the ablated surface particles, and from the measured data, an absorption coefficient was inferred. At intensities greater than $10^{9}W/cm^{2}$ the transmitted beam showed a cutoff approximately 25 nsecs after the start of the laser pulse, indicative of the formation of an overdense plasma. All reflection measurements showed that the scattering was primarily specular. At intensities between 10^{8} and $10^{9}W/cm^{2}$, the reflected beam exhibited a narrow pulse attributable to thermal damage at the target surface. At intensities of $10^{9}W/cm^{2}$ or greater, the reflected beam also indicated a sharp decrease in amplitude attributed to absorption in the newly-formed plasma. The value of the absorption coefficient was calculated to be 0.545.

TABLE OF CONTENTS

I. INTRODUCTION---------- 8

II. THEORY---------- 11

III. EXPERIMENTAL ARRANGEMENT---------- 19

A. LASER---------- 19

B. LASER MONITORING TECHNIQUES---------- 19

C. VACUUM CHAMBER---------- 20

D. TRANSMISSION AND DETECTION SIGNAL ARRANGEMENT ARRANGEMENT---------- 20

IV. TRANSMISSION EXPERIMENTS---------- 22

V. REFLECTION AND ABSORPTION---------- 27

VI. DISCUSSION---------- 30

VII. SUMMARY AND CONCLUSIONS---------- 40

VIII. RECOMMENDATIONS REGARDING FURTHER RESEARCH---- 42

BIBLIOGRAPHY---------- 64

INITIAL DISTRIBUTION LIST---------- 67

LIST OF FIGURES

1. Incident frequency matching plasma frequency in the linear region of electron density profile.

2. Dependence of the reflection coefficient on the flux density for aluminum.

3. Block diagram of the general experimental layout.

4. Top view of vacuum chamber.

5. Arrangement for making reflection and transmission measurements.

6. Power transmitted vs time as a function of power density.

7. Laser power and transmitted power vs time for P_D = $8.1 \times 10^8 W/cm^2$.

8. Laser power and transmitted power vs time for P_D = $1.1 \times 10^9 W/cm^2$.

9. Laser power and transmitted power vs time for P_D = $1.5 \times 10^9 W/cm^2$.

10. Laser power and transmitted power vs time for P_D = $4.1 \times 10^9 W/cm^2$.

11. Laser power and transmitted power vs time for P_D = $6.7 \times 10^9 W/cm^2$.

12. Laser power and transmitted power vs time for P_D = $7.3 \times 10^{10} W/cm^2$.

13. Laser power and transmitted power vs time for P_D = $8.0 \times 10^{10} W/cm^2$.

14. L_N time to cutoff, t_o, vs l_n power density.

15. Representative laser power pulse during reflection measurements.

16. Reflected power vs time for power densities above and below plasma threshold.

17. Reflected power vs time for $P_D = 6.6 \times 10^8 W/cm^2$.

18. Reflected power vs time for $P_D = 7.4 \times 10^8 W/cm^2$.

19. Reflected power vs time for $P_D = 7.1 \times 10^8 W/cm^2$.

20. Reflected power vs time for $P_D = 3.8 \times 10^9 W/cm^2$.

21. Reflected power vs time for $P_D = 5.7 \times 10^{10} W/cm^2$.

I. INTRODUCTION

By focusing a giant pulse Q-switched laser onto an opaque solid material, a hot dense plasma may be formed. The initial energy in the pulse vaporizes and ionizes the surface atoms, while the remaining energy may continue to heat, and further ionize, the ablated particles.

Considerable attention has recently been directed toward laser energy deposition in a solid material and the resultant plasma. The effective target damage is of interest in the first case, while the second case has significance for the possible occurrence of nuclear fusion by compression.

Basov and Krokhin (Ref. 1) were the first to consider the possible use of lasers to achieve thermonuclear fusion. They were followed by Dawson (Ref. 2), and in much more detail by Hertzberg et al. (Ref. 3). Brueckner and Jorna (Ref. 4) gave a detailed analysis of the present state of the art of laser-driven fusion with respect to D-T pellet compression. In both cases, however, whether they require the enormous intensities for thermonuclear fusion, or the lesser intensities for material damage studies, the coupling of the incident energy into the irradiated material and the subsequent plasma is of prime importance.

Laser irradiances incident upon a solid target will deposit a fraction of the energy into heating of the target

surface, while the remaining energy is reflected, or absorbed by the resultant plasma. The temperature rise of the solid at the surface can be predicted by using the heat equation for a semi-infinite solid;

$$T = \frac{2(1-R)F_0}{K} (Dt/\pi)^{\frac{1}{2}} \qquad (1)$$

where R is the surface reflectivity, F_0 is the laser irradiance, K is the thermal conductivity, D is the thermal diffusivity, and t is the laser pulse time.

The thermionic emission of electrons and ions from the surface material may be estimated by using Richardson's equation;

$$J = AT^2 \exp(-\phi/kT) \qquad (2)$$

where A is a constant, T is the electron or ion temperature, ϕ is the ion or electron work function, k is Boltzmann's constant, and J is the electron or ion current. Therefore, the amount of thermal electron or ionic emission increases rapidly with increasing temperature, and from Eqn. (1), the temperature is proportional to the incident laser irradiance.

When the laser irradiance is above a certain threshold, a very dense, hot, ionized plasma is formed; and unique phenomena not observed during thermionic and ionic emission processes occur. These phenomena are associated with the transmission, absorption, and reflection of electromagnetic waves, in or at the boundary of, the laser-produced plasma.

The degree of ionization is given by the Langmuir-Saha equation;

$$i/i_o = (g/g_o)\exp(\phi-I)/kT \qquad (3)$$

where i, i_o are respectively the ion and neutral molecule fluxes, g, g_o are the statistical weights of the ionic and neutral states, ϕ is the electron work function, and I is the ionization potential. Thus, at high laser irradiances the material ejected from the solid surface is almost fully ionized, while at lower irradiances a fraction of neutral molecules is ejected. Ready (Ref. 5) described an experiment in which a ruby laser with an irradiance of $10^9 W/cm^2$ vaporized a thin aluminum target. Through the analysis of charge collection data, the ionization efficiency was determined to be 1%. Brooks (Ref. 6) from measurements of his charge collection data in a similar experiment, determined the ionization efficiency to be 10%.

Thus, thermal electrons, ions, and neutral molecules are the cardinal particulates encountered with the laser irradiances of interest. The purpose of this thesis is to examine the interaction of the laser photons with the target and the vaporized electrons, ions and neutral molecules. In particular, an attempt will be made to establish a time profile of the laser flux from the time it irradiates the target until its extinction. In addition, a spatial profile will be developed for the particle distribution and the direction of the scattered laser flux.

II. THEORY

Using the equation for the temperature rise of a semi-infinite solid, Eqn. (1), one finds that the threshold for thermionic emission for an aluminum target is $2 \times 10^8 W/cm^2$. Above this threshold, up to $10^9 W/cm^2$, the electrons and ions interact as independant particles. In this power density regime, the stream of ablated particles is essentially transparent to 1.06 μ radiation, and thus no appreciable scattering or absorption of the incident radiation should occur. Except for losses due to the initial heating of the material, the laser pulse should not undergo any spatial or temporal changes in passing through the stream of particles. Also, the specularly reflected pulse, after accounting for changes of reflectivity due to the temperature rise at the surface of the target, should show no spatial or temporal deviations from the incident laser pulse.

At power densities greater than $10^9 W/cm^2$, collective behavior of the much denser ions and electrons, instead of their independent behavior, becomes dominant. The absorptive and reflective processes no longer are negligible. It is at this threshold that the vaporized material becomes a hot, dense, ionized, hydromagnetically turbulent plasma.

The precise mechanisms for formation of the plasma are not generally understood. However, a theoretical parameter which measures the degree to which collective effects dominate

individual particle effects is given by the Coulomb Cutoff Parameter defined as;

$$\Lambda = \lambda_c/\lambda_d \tag{4}$$

where λ_c is,

$$\lambda_c = 1/4\pi R_c^2 N \qquad \text{(cgs)}$$

and λ_d, the Debye length, is,

$$\lambda_d = (kT/M)^{\frac{1}{2}}(1/\omega_p) \qquad \text{(cgs)} \tag{5}$$

If an ionized gas is not to recombine, then the average kinetic energy, $<kT>$, must be greater than the average potential energy, $<q^2/R>$. R_c is defined as that distance at which the average kinetic energy is equal to the average potential energy, or;

$$R_c = q^2/kT. \qquad \text{(cgs)} \tag{6}$$

ω_p is the plasma frequency and is defined as;

$$\omega_p = (4\pi Nq^2/M)^{\frac{1}{2}} \qquad \text{(cgs)} \tag{7}$$

where N is the average density, and M is the mass of the particle of interest.

After substituting Eqns. (5), (6), and (7) into Eqn. (4), we find that for electrons:

$$\Lambda = 1.23 \times 10^7 T_E^{\,3/2}/N_E^{\frac{1}{2}}$$

where T_E is the electron temperature in degrees Kelvin, and N_E is the electron density per cubic meter. For a plasma,

Λ is much greater than one. At intensities of $10^9 W/cm^2$ or greater, sufficient electron densities and temperatures are achieved to satisfy this inequality and collective particle behavior dominates.

Once the plasma is formed, it rapidly expands. Smith and Fowler (Ref. 7) indicate that the plasma propagates up the laser beam to a point where the laser intensity is just sufficient to overcome the losses. The principle loss mechanism is bremsstrahlung due to electrons accelerating in the fields of ions. The electron-electron interactions are negligible. Dawson (Ref. 8) derived the total radiation emitted per unit volume and it is given by;

$$P_T = (16\pi^2 z^2 e^6 N_E / 3c^3 M_E h)(kT_E / M_E). \qquad (8)$$

He later showed that for laboratory size plasmas this radiation loss is small. Therefore, according to Smith and Fowler, the plasma would expand initially up the laser beam until the radiation loss rate equalled energy input. As the plasma expanded up the beam it would effectively shield the target from the laser irradiance either by absorption or refraction due to the large density gradients at the leading plasma edge.

Brooks (Ref. 6) irradiated an aluminum target at a power density of $10^9 W/cm^2$, sufficient to create plasma. The radiation was incident at an angle 30° from the target normal. Probe instruments indicated the creation of two plasma fronts. The earlier, smaller disturbance propagated in the specular

direction 30^{o} from the target normal at a speed of 1.1 x 10^{8}cm/sec. The later disturbance, identified as the main plasma, propagated initially in the specular direction at a speed of 1.1 x 10^{7}cm/sec. At times after the expiration of the laser pulse, the main plasma propagated in a direction normal to the target. Brooks' measurements apparently contradict those of Smith and Fowler. However, Brooks was not able to make measurements in the path of the beam due to the obvious laser influence on the probes. Thus, a critical density gradient in the incident direction might have existed that was undetectable by Brooks. However, as will be discussed later, a large density gradient does not need to be anti-parallel to the incident laser beam to effectively shield the target. Theoretically, density gradients in the specular direction could shield the target and account for cutoff of the laser beam. In any event, a model will be proposed later to match the theory of Smith and Fowler to the findings of Brooks.

The target shielding mechanisms are reflection and absorption. The threshold for these mechanisms to become dominant is a function of the particle densities in the plasma. Complete cutoff of electromagnetic radiation at a specific wavelength will occur when the radiation frequency is equal to the plasma frequency; that is, when,

$$\omega_L = \omega_p = (4\pi Nq^2/M)^{\frac{1}{2}}.$$

The critical density for electrons with electromagnetic radiation at 1.06 μ is on the order of 10^{21} particles per cubic cm.

Dawson et al. (Ref. 9) showed the effect of a density gradient upon the absorption coefficient prior to cutoff of the electromagnetic radiation. The absorption coefficient for a plasma is given by;

$$K = \omega_p^2/c\omega\tau(\omega^2-\omega_p^2)^{\frac{1}{2}} \tag{9}$$

where τ is the electron-ion collision time and is given by;

$$\tau = 2.4 \times 10^4 \, T_E^{\,3/2}/N_E Z. \tag{10}$$

N_E is the electron density per cm^3, Z is the nuclear charge, and T_E is the electron temperature in electron volts. As ω approaches ω_p, the absorption coefficient becomes quite large. This is physically reasonable since as the electromagnetic wave frequency becomes close to resonance with the plasma frequency, the wave is more likely to be absorbed.

Dawson calculated the total absorption coefficient by integrating from a point outside the plasma to point R where $\omega_L = \omega_p$. R is defined as the density fall-off distance and is illustrated in Fig. (1). Dawson's integral to be evaluated is;

$$K_T = 2\int_{-\infty}^{R} \frac{\omega_p^2(x)\,dx}{c\omega\tau(x)(\omega^2-\omega_p^2)^{\frac{1}{2}}}. \tag{11}$$

The integral was multiplied by 2 to account for the reflected beam. Assuming a linear density gradient, the solution to Eqn. (11) is;

$$K_T = \frac{32}{15} \frac{R}{c\tau(R)} \tag{12}$$

and the fraction of energy reflected is;

$$I_R/I_O = \exp(-K_T). \tag{13}$$

Therefore, considerable absorption will take place if R is greater than $c\tau/2$. If one assumes an electron temperature of 3 eV and an average ionic charge of 3 in the early plasma, then R must be greater than $6.1 \times 10^{14}/N_E$ in order to have appreciable absorption.

For the case of a finite density gradient, absorption may take place in a laboratory plasma with densities of the order of $10^{21}/cm^3$. However, if the gradient approaches a discontinuity such that R approaches zero, almost total reflection would be predicted.

Dawson's calculations were based upon normal incidence. Shearer (Ref. 10) included the effect of oblique incidence on the absorption of an electromagnetic wave. His analysis was similar to that of Dawson. Shearer's total absorption coefficient is given by;

$$K_T = \frac{32}{15} \frac{K_o N_c^2 \cos^5\theta}{\nabla N_E}$$

where K_o is;

$$K_o = (4/3(2/\pi M_E)^{\frac{1}{2}}e^4/c)Z/(kT_E)^{3/2}Ln\Lambda$$

In Eqn. (14), N_c is the critical density at which $\omega_L = \omega_p$, and θ is the angle between the incident electromagnetic wave and the plasma density gradient vector.

By examining Eqn. (14), one can see the angular effect on the total absorption coefficient. For maximum absorption, the angle between the incident wave and the plasma density gradient vector should be kept less than 30^o.

Also, the effect of the density gradient itself can be seen. Like Dawson's analytical results, if the density gradient is very large, then almost all of the incident wave will be reflected. Table (1) shows the fraction of energy reflected for various density gradients as calculated from Eqn. (14) when applied to aluminum.

TABLE 1.

$\nabla N_E (cm^{-4})$	I_R/I_O
10^{26}	0.99
10^{25}	0.91
10^{24}	0.40
10^{23}	0.00

Basov et al. (Ref. 11) experimentally showed the reduction of the reflection coefficient of a solid as a function of laser flux intensities. A sharp reduction occurred at intensities of $10^9 W/cm^2$. Their findings are shown in Fig. (2). They attributed the sharp reduction to the formation of a transition layer in the surface material, consisting of

a plasma in hydrodynamic motion with a length comparable to that of the mean free path of a photon in the layer. Their result also implies the effect of a density gradient on the amount of reflected radiation.

In summary, at radiation densities of $10^8 W/cm^2$ or greater, the energy absorption at the target is sufficient for heating a surface layer of thickness about 10^{-4} to 10^{-5}cm, the mean free path of a laser photon, which is on the same order as the 1.06 μ radiation wavelength. At power densities of $10^9 W/cm^2$ or greater, a dense plasma in a state of hydrodynamic motion is formed which effectively shields the target. The shielding of the target is a function of the reflection and absorption from the transition layer of the plasma. Reflection and absorption are functions of the length of the layer and the particle density distributions. The density distributions are related to the material parameters of the target and the incident photon flux.

III. EXPERIMENTAL ARRANGEMENT

A. LASER

The laser used in this investigation was a Korad K-1500 Q-switched Neodymium doped-glass laser system. The system consisted of an oscillator (K-1) which generated the giant 25-30 nsec pulse (full width at half maximum) after Q-switching through a Pockels Cell. The output beam is then expanded by expansion optics from the 1.27 cm diameter of the K-1 laser rod to the 1.90 cm diameter of the amplifier (K-2) rod. The arrangement of the laser components is illustrated in Fig. 3. The output pulse energy of the laser can be varied from 3.0 to 12.0 joules by varying the control voltages to the flashlamps of the K-1 and K-2 heads. A more detailed description of the laser system can be obtained in Ref. (12).

B. LASER MONITORING TECHNIQUES

In order to monitor the laser beam, a Korad KD-1 photodiode was used. Approximately 8% of the laser beam was reflected from a glass slide beam splitter to a magnesium oxide diffusion block. The beam then passed through 0.1% neutral density filter to the KD-1 photodiode.

The KD-1 photodiode provided two signals: one proportional to the laser energy, another proportional to the laser pulse power. The photodiode energy signal was calibrated using a Korad KJ-3 calorimeter. The calorimeter was used to

provide an absolute measure of the laser energy against which the voltage on a Tektronix 7904 storage oscilloscope which displayed the energy signal could be calibrated. The power output was read on a Tektronix 7904 oscilloscope.

C. VACUUM CHAMBER

A schematic of the vacuum chamber is given in Fig. (4). The target used was a 1 mm thick aluminum alloy plate. The beam entered the chamber entrance window and was incident on the target at an angle 30^{o} to the target's normal. A 0.048 cm diameter hole was drilled through the target to allow passage of some of the incident radiation prior to cutoff. The target was mounted on a .635 cm backing plate with a 0.95 cm diameter hole drilled through it.

The power densities at the target were altered by varying the laser energy or changing the focusing lens. The target was located 27 cm from the focusing lens. The focal lengths of the lenses used throughout the experiment were 28, 31, and 40 cm. These focal lengths gave spot sizes of .004, .048, and .306 cm^2 respectively. Therefore, by varying the laser energy and the focusing lenses, the power densities at the target could range from 10^8 to $10^{10} W/cm^2$.

D. TRANSMISSION AND DETECTION SIGNAL ARRANGEMENT

The schematic for the signal detection system is shown in Fig. (5). Both the reflected and transmitted signals were detected by an ITT photocell similar in performance to the KD-1 photodiode. Since only one detector was available,

the reflection and transmission signals could not be detected simultaneously. Other detectors exhibited an unsatisfactory fall-off time which was critical in this experiment.

The transmitted, or reflected signal, after exiting the vacuum chamber, was reflected from a glass slide beam splitter to a magnesium oxide diffusion block. The transmitted signal would exit the chamber via window no. 3, while the reflected signal would exit the chamber through windows no. 2, 5, or 6. The signals would then pass through a 1.06 μ line filter in order to eliminate detection of plasma radiation at other wavelengths. The line filter was mounted at the entrance to the ITT photocell. The power output was displayed on a Tektronix 7704 oscilloscope triggered by the output signal of the KD-1 photodiode.

In order to eliminate detection of unwanted multiple reflection signals in the desired transmitted laser signal, a collimating cone surrounded the beam after it passed through the target hole. Similarly a circular plate with a 1.90 cm diameter hole was inserted inside the chamber windows to eliminate unwanted multiple reflection signals from the reflection laser signal.

The chamber was evacuated to a pressure of 3×10^{-6} Torr with an oil diffusion pump. The vacuum pressures were measured with an ionization guage.

IV. TRANSMISSION EXPERIMENTS

Prior to measurement of laser transmission as a function of power density at the target, absorptive and reflective energy losses through the glass slide beam splitter, entrance window, and the focusing lenses were determined. This was accomplished by inserting a Hadron thermopyle directly in the path of the laser beam, but behind each of the components being considered. The output of the thermopyle, which was proportional to energy, was sent directly to a milli-microvoltmeter which was linked to a HR-96 X-Y recorder. The output of the recorder was compared to the energy output of the KD-1 photodiode as read on the storage oscilloscope. The losses through the entrance window and beam splitter were determined to be 12% of the initial laser energy. Losses through the various lenses averaged 3% giving a total loss of 15% of the initial laser energy.

The laser energy, as read on the storage oscilloscope, was multiplied by a factor of 0.85 in determining the power density at the target surface. The power density was calculated by;

$$P_D = 0.85\ E_L/A_S t_P$$

where E_L is the initial laser energy, A_S is the area of the focused spot size on the target, and t_p is the half width of the laser pulse. As indicated in Sec. III, the power density

could be varied by changing either the laser energy or the area of the focal spot. Near the end of the experiments the adjustability of laser energy was lost due to an apparently failing flashlamp in the K-2 amplifier. Consequently, only the focusing lens could alter the power density and as a result, the range of power densities became a series of steps, instead of a smooth curve. However, power densities above and below the plasma threshold were obtainable.

The laser and transmitted power signals as functions of time were read on adjacent oscilloscopes as depicted in Fig. (5). While attempting to establish a true time relationship between the laser and transmitted pulses, a 70 nsec delay was discovered in the slower oscilloscope on which the transmitted signal was to be read. This was verified, after including geometrical and cable delays, by simultaneously observing the laser pulse on both of the oscilloscopes. Further verification was obtained by double exposing two laser pulses, one detected with the KD-1 photodiode, and the other detected with the ITT photodiode. The double exposure showed only the 12 nsec built-in cable delay.

However, the start of the pulse on the slower oscilloscope appeared to begin earlier with increasing laser power. Although a t_o for the pulse on the slower oscilloscope could be calculated from previous measurements at nearly constant power, it could not be relied upon at other laser powers. Consequently, t_o for the transmitted pulse, and also in later

reflection measurements, was determined to be the beginning of the pulse as observed on the oscilloscope.

The initial series of measurements was made while the chamber was at atmospheric pressure. The power density at the target was varied from 10^8 to $10^{10}W/cm^2$. In all cases, cutoff of the transmission pulse prior to expiration of the laser pulse was observed. This indicated that at power densities as low as $10^8W/cm^2$, a plasma was being formed and the laser energy was being absorbed or reflected.

The threshold for breakdown of air at atmospheric pressure is given by Ready (Ref. 5) at $10^{11}W/cm^2$. The diffraction-limited spot size for the lenses in use was calculated to be on the order of $10^{-3}cm$. Therefore, even after passage through the 0.050 cm hole, sufficient intensities were obtained at the focal spot behind the target to cause air breakdown. Air breakdown was apparently the mechanism causing the cutoff of the laser radiation. This was verified by not focusing the laser beam and noting the perfect matching between the laser beam and the transmitted beam.

To avoid the problem of air breakdown, the chamber was evacuated to a pressure of 3×10^{-6} Torr. Measurements were then taken of the transmission pulse covering the range from 10^8 up to $10^{10}W/cm^2$. Fig. (6) compares several transmission pulses as a function of time for several power densities. The duration of the laser pulse was from 70-80 nsecs. The data depicted in Fig. (6) are representative of many other measurements taken during the experiment.

Cutoff is shown to occur only at those power densities greater than $10^9 W/cm^2$. At densities below this, cutoff does not occur and is consistent with the theory presented in section II.

Figs. (7)-(13) compare the history of the laser pulse and the transmitted pulse as a function of time. The amplitudes of the transmission pulse are not drawn to scale and serve only to compare the time history of the two pulses. The absorption and reflection phenomena become predominant between 20 and 30 nsecs after the beginning of the laser pulse. The decrease in the time required to reach onset as power increases is consistent with the time dependence upon $(P_D)^{-2}$ from the heat equation for semi-infinite solids (Eqn. 1). Using Eqn. (1) and rearranging, an estimate of the time required for the absorption and reflection phenomena to occur can be made. After inserting the ionization temperature for aluminum of $60,000^{\circ}$ Kelvin, and a power density of $1.1 \times 10^9 W/cm^2$, the required time is estimated as 9 nsecs. This is in good agreement with Fig. (8). However, at higher power densities, the time becomes too short to be measured due to the $(P_D)^{-2}$ dependence.

To summarize the transmission experiment, a cutoff of the laser radiation was observed to occur at power densities greater than $10^9 W/cm^2$. This indicates that an overdense plasma (density greater than $10^{21}/cm^3$ for 1.06 μ radiation) is being formed. Since the cutoff is complete, the overdense plasma

exists for as least as long as the laser pulse. In addition, the formation of the overdense plasma begins to occur 20 - 30 nsecs after the laser pulse depending upon the power density at the target.

V. REFLECTION AND ABSORPTION

In order to first establish the primary direction of the reflected (scattered) radiation, measurements were taken at 0^{o}, 30^{0} (specular) and 75^{o} from the target normal. This corresponds to window nos. 2, 5, and 6 in Fig. (4). Measurements were taken below and above the experimentally determined plasma threshold. Table (2) summarizes the results.

TABLE 2.

Angle	Threshold	Signal Strength
0	above	0.25 V
0	below	0.65
30(specular)	above	1.40
30(specular)	below	4.60
75	above	0.16
75	below	0.40

The results indicate that approximately 80% of the scattered laser radiation is in the specular direction. In addition, there is approximately 3 times more radiation scattered below threshold, than above. This is consistent with the results of Basov *et al*. (Ref. 11) and will be treated in more detail later.

Measurements were then taken of the scattered radiation solely in the specular direction at power densities ranging from 10^{8} to $10^{10} W/cm^{2}$. Fig. (15) gives the time history of

a typical laser pulse. Fig. (16) gives a comparison of a typical reflected pulse above and below plasma threshold. In all cases, the reflected pulse was from 4 - 6 nsecs narrower at half maximum and in several cases appeared to exhibit cutoff. The narrow width and evidences of cutoff indicated formation of an overdense plasma below plasma threshold similar to the air breakdown problem associated with the transmission experiment. To check this possible interpretation adequacy of the vacuum 3 x 10^{-6} Torr maintained in the chamber to completely eliminate air breakdown was considered.

Ready (Ref. 5) describes gas breakdown as occurring in two stages. The first stage consists of pre-ionization of the gas molecules while the second stage consists of a cascade, or avalanche, of ionization. It is during this latter phase that the heavy absorptive, or cutoff phenomenon occurs. However, at operating pressures of 10^{-3} Torr and below, the avalanche ionization will not occur and the cutoff phenomenon will not be observed.

The initial ionization phase is considered to occur primarily by multiphoton absorption. Bystrova *et al.* (Ref. 13), Voronov *et al.* (Ref. 14), and Delone *et al.* (Ref. 15) conducted experiments of multiphoton absorption of laser light at pressures of 10^{-4}, 10^{-4}, and 10^{-5} Torr respectively. In particular, Voronov conducted an experiment using a ruby laser with $\hbar\omega$ equal to 1.73 eV, and H_2 molecules with an ionization potential of 15.43 eV at an operating pressure of 10^{-4} Torr.

Since the Nd laser, with $\hbar\omega$ equal to 1.18 eV and N_2 molecules (prime constituent of air) with an ionization potential of 15.43 eV, were close to the parameters used by Voronov et al., a rough comparison with their data was made to obtain an estimate of the magnitude of the multiphoton absorption process in the current experiment. The results indicated that the magnitude of multiphoton absorption is negligible and, therefore, some other mechanism must be causing the narrowing of the reflected pulse.

Figs. (16) - (21) illustrate the time histories of reflected laser pulses. The narrowing and cutoff of the reflected pulses can be readily observed. In addition, a marked decrease in amplitudes of the reflected pulses above plasma threshold can be seen in Fig. (16). This was previously observed in the specular portion of the experiment. Finally, the peaks of the reflected pulses above plasma threshold correspond to the peaks of the previously measured transmitted pulses. The peaks of the transmitted pulses signified the beginning of the reflective and absorptive processes in the plasma. Therefore, it appears that, perhaps, the absorptive phenomena become dominant since the reflected and transmitted pulses have passed their maxima. However, the peak of the reflected pulse below plasma threshold, when the reflection can be assumed to entirely from the metal, also falls into this range. More will be said about this later.

VI. DISCUSSION

The observed cutoff of the transmitted laser radiation at power densities greater than $10^9 W/cm^2$ verifies the formation of an overdense plasma somewhere in the path of the laser beam. The data show that the reflective and absorptive processes commence between 20 to 30 nsecs after the beginning of the laser pulse depending upon the incident flux. The threshold of $10^9 W/cm^2$ for plasma formation agrees with theory, while the time for the absorptive and reflective processes to occur at $10^9 W/cm^2$ agrees with that predicted by the heat equation for a semi-infinite solid. The time has an inverse square dependence upon power density and therefore could not be resolved by the detectors at higher powers. However, Figs. (8) - (13) indicate earlier onsets of absorption or reflection for increasing power densities as predicted by the heat equation. Fig. (14) is a plot of the time to cutoff, t_o, as a function of the reciprocal of the power density squared.

However, there are two results that require further examination before any conclusions can be inferred. The first of these is associated with the narrowing and eventual disappearance of the reflected pulse, while the second is associated with the direction of the critical density gradient and the measured reflection data.

The narrowing of the reflected pulse at power densities below plasma threshold may be attributed to the reduction of the reflection coefficient experimentally determined by Basov et al. (Ref. 11). At power densities greater than $10^9 W/cm^2$, the reflection coefficient continues to drop. The continued reduction of the reflection coefficient at power densities greater than $10^9 W/cm^2$ has been attributed to the formation of a transition layer consisting of a dense plasma. The dependence of the reflection coefficient upon the power density is given for aluminum in Fig. (2). At lower power densities, the value of the reflection coefficient is close to the reflection coefficient for non-disturbed surfaces. For aluminum, the value is about 0.80. As the power density increases, the reflection coefficient decreases due to thermally-induced damage to the aluminum target.

Fig. (18) shows the reflected signal for a power density of $7.4 \times 10^8 W/cm^2$. According to Basov et al., this would correspond to a reflection coefficient of approximately 0.50 as compared to the reflection coefficient of 0.80 for an undisturbed surface. The rise time of the laser pulse is 35 nsecs while the rise time of the reflected pulse is about 22 nsecs. If the pulse in Fig. (17) were allowed to rise the full 35 nsecs, its amplitude would almost double, and its half width would approach that of the laser pulse. The full 35 nsec rise time resembling the laser pulse would correspond to a lower power density and the reflection coefficient for

an undisturbed surface. Therefore, the narrowing of the reflected pulse below threshold is apparently attributable to the reduction of the reflection coefficient due to thermal damage, previously determined by Basov et al.

The further reduction of amplitude and eventual disappearance of the reflected pulse above plasma threshold may be due to absorption in the plasma, or redirection of the laser beam away from the detector by the rapidly expanding plasma. In the first case, Basov et al. showed that the reflection coefficient continues to decrease at power densities greater than $10^9 W/cm^2$. The reduction of the reflection coefficient was attributed to the formation of a transition layer consisting of a dense absorbing plasma. The length of the transition layer was predicted to be on the order of a mean free path of a photon in a solid, or approximately 10^{-4} to 10^{-5}cm. Additionally, Dawson (Ref. 9) predicted an absorption coefficient of unity if the density fall-off distance was on the order of $c\tau/2$ where τ is the electron-ion collision time.

The measured reflection signal from a plasma in this experiment averaged 40 mV according to Figs. (16), (20), and (21). The measured reflection signal below plasma threshold was 80 mV. However, between $7.4 \times 10^8 W/cm^2$ and $10^9 W/cm^2$, taken as plasma threshold, the reflection coefficient decreases approximately 15%. Taking this into consideration and since the reflection of the signal below plasma threshold can be assumed to be entirely from the solid target, the 40 mV signal implies that 42% of the energy is absorbed in the plasma,

scattered at other angles, or scattered at other frequencies. Ignoring the last two, this value is in close agreement with the observations of Basov, illustrated in Fig. (2). The fraction of reflected energy after plasma formation is, therefore, 58%. Since $I_R/I_O = \exp(-K_T)$, $K_T = 0.545$.

Basov's model produced a continuous curve for the reflection coefficient as a function of power density from 10^7 to $10^{11} W/cm^2$. The model does not appear realistic in that a discontinuity should arise during the transition from the solid state to the gaseous plasma state. Nevertheless, the Basov mode will continue to be used as a means to estimate the absorption coefficient.

To obtain an estimate of the characteristic density fall-off length, Dawson's (Ref. 9) formula may be used:

$$R = \frac{15}{32} c\tau(R)K$$

where τ, the electron-ion collision time is

$$\tau = \frac{2.4 \times 10^4 T_E^{3/2}}{N_E}$$

Brooks estimated that 1.7×10^{19} atoms were ejected from the target surface per laser shot. Assuming a 10% ionization efficiency and an average ionic charge of 3, this yields a total of 5.1×10^{18} electrons. The volume of the crater was measured with an electron microscope after 50 shots and was found to be 0.014 cm^3. This gives an electron density of $1.8 \times 10^{21}/cm^3$. Therefore,

$$R = 2.18 \times 10^{-7} T_E^{3/2}$$

For $T_E = 3$ eV, $R = 1.1 \times 10^{-5}$ cm

For $T_E = 30$ eV, $R = 3.5 \times 10^{-5}$ cm.

The latter result for T_E equal to 30 eV corresponds to Basov's theory that the transition layer of the plasma is on the order of the mean free path of a laser photon. Also, the 42% reduction in the amount of reflected light above plasma threshold is consistent with Basov's experiment and with Dawson's theory.

In addition, Lubin et al. (Ref. 16) derived an equation for the skin depth of a solid by using an absorption coefficient that was a function of the electron collision time, an effective plasma frequency, and the laser frequency. The resulting equation was;

$$\partial = \frac{\lambda}{4\pi K_T}$$

For $K_T = 0.545$, the skin depth would be approximately 1.5×10^{-5} cm, or on the order of the mean free path of a photon as predicted by Basov, and the value of the calculated density fall-off distance for an electron temperature of 30 eV from the data in this experiment.

As indicated earlier, however, disappearance of the reflected pulse could be attributed to redirection of the reflected beam by the rapidly expanding plasma front. Since

the reflection of the beam was determined to be primarily specular, the 1.90 cm diameter collimator was removed from the chamber in order to determine if the beam was being redirected out of the collimator. The measurements taken after removal duplicated the original measurements and the disappearance phenomenon was again observed.

In an effort to determine if the reflected beam was being redirected out of the exit window and into the chamber wall, Hadron laser footprint paper was attached inside the chamber to the exit window. After 20 laser shots, the paper was examined, but no burn pattern was observed so the experiment was abandoned.

Since the experiment with the footprint paper was uninformative, an attempt was made to analyze the motion of the plasma from the data of Brooks to determine if the reflected beam was being redirected into the chamber wall.

Brooks determined that the speed of the early plasma was 1.1×10^{8} cm/sec. This was an asymptotic solution and therefore the speed of the early plasma would be somewhat greater nearer the target. Since the speed of the early plasma was one order of magnitude greater than the speed of the main plasma, the early plasma was considered to be the primary mechanism associated with the reflection or redirection of the laser light.

If the early plasma propagated as a slab in a direction along the target normal, its critical density layer would have to travel 2 cm in order to walk the reflected beam out

of the exit window and into the chamber wall. Total disappearance of the laser pulse occurs approximately 20 nsecs after plasma formation. This was determined by matching the reflected pulse to the transmitted pulse. Brooks' density contours for the early plasma show an underdense plasma 2 cm along the normal to the target after 25 nsecs. Nowhere in his density contours is there evidence of an overdense reflecting plasma at a position 2 cm along the normal to the target when the disappearance of the reflected pulse was observed. Therefore, a plasma with a critical density layer propagating as a slab normal to the target surface could not be the mechanism causing the disappearance of the reflected pulse.

The development of a critical density layer propagating in the direction of the laser beam could effectively direct the beam away from the target wall and toward the backscattered direction. Brooks' density contours for the early plasma do not show any critical density layers. A critical density layer could be propagating up the laser beam as indicated by Smith and Fowler or it could remain within a few mean free paths of the laser photons in the solid target. Brooks' density mapping taken 10 nsecs after plasma formation was the earliest he could obtain. This mapping indicates an underdense contour slightly off perpendicular to the incident beam. At 20 nsecs this density contour appears to have moved more toward the perpendicular direction. By crudely extrapolating back to the target, a critical density layer can be imagined with its plane perpendicular to the laser beam.

The development of this layer could effectively redirect the beam out of the window and cause the disappearance of the laser pulse.

The second phenomenon to be examined is the specular scattering data and how it relates to a critical density gradient compatible with the findings of Brooks. The cutoff of the laser radiation observed during the transmission measurements is consistent with the theory of Smith and Fowler (Ref. 7) that the plasma propagates along the laser beam up to the point where the laser energy is insufficient to overcome the plasma losses by bremsstrahlung. With the losses by bremsstrahlung, through electron-ion interactions being small in laboratory plasmas, complete cutoff of the 30 nsec pulse would be predicted and was observed as shown in Figs. (8) - (13).

However, Brooks' data show that the early plasma accelerated in the specular direction. Assuming that the driving force is a pressure gradient and using the ideal gas law, the pressure gradient may be written:

$$\vec{\nabla}P = kT\vec{\nabla}N + kN\vec{\nabla}T \quad . \tag{15}$$

Wegener (Ref. 17) studied the spontaneous magnetic field associated with a laser-produced plasma. The source term for the magnetic field is given by Schwirzke (Ref. 18);

$$\nabla x \frac{1}{Ne} \vec{\nabla}P = \nabla x \frac{1}{Ne} \vec{\nabla}(NkT) = \nabla x \left(\frac{k}{e}\vec{\nabla}T + \frac{kT}{Ne}\vec{\nabla}N\right) \tag{16}$$

Since the temperature is a scalar, and the density gradient is a vector, the following vector identity applies;

$$\nabla x(a\vec{B}) = a\nabla x\vec{B} = \nabla a x\vec{B}$$

Using this identity and the fact that the curl of a gradient is zero, the source term, Eqn. (16) reduces to:

$$\vec{S} = \frac{k}{e}\vec{\nabla T} \; x\frac{l}{N}\vec{\nabla N} \qquad (17)$$

Since $\vec{S}$ is known not to be zero, $\vec{\nabla T}$ and $\vec{\nabla N}$ cannot be in the same direction.

The plasma would be accelerated in the direction of the largest pressure gradient and, as found by Brooks, in the specular direction. The pressure gradient is the sum of the temperature and density gradients, and the temperature gradient is largest in the radial direction as indicated by Wegener (Ref. 17). Therefore, the density gradient associated with this temperature gradient cannot be in the specular direction. It would be expected, therefore, that the density gradient connected with the acceleration of the early plasma would point somewhere between the specular direction and anti-parallel to the incident beam.

As indicated earlier, Shearer (Ref. 10) showed the effect of oblique incidence of the laser radiation upon the absorption coefficient of the plasma. In short, the total absorption coefficient is proportional to $\cos^5\theta$ where θ is the angle between the incident wave vector and the density gradient vector. If the density gradient containing the critical

density layer is assumed to produce the largest pressure gradient, then some indication of its direction can be obtained from the measured reflection data.

The observed absorption coefficient was 0.545. If the critical density gradient were directed close to specular, the total absorption coefficient would have been reduced 97% from that of normal incidence. This is inconsistent with the observed data. If the density gradient were pointed in the target normal direction, the total absorption coefficient would have been reduced 53%. This would give an absorption coefficient of about 1.09 for normal incidence. This would be compatible with anticipated values of the total absorption coefficient for the characteristic density falloff length of 10^{-5} to 10^{-6} cm, a critical density of $10^{21}/cm^3$, and an assumed electron temperature of 30eV.

VII. SUMMARY AND CONCLUSIONS

The cutoff of the transmitted laser radiation at power densities greater than $10^9 W/cm^2$ verifies the formation of an overdense plasma with a critical density layer somewhere in the path of the incident beam. At this point, the plasma shields the target from further laser irradiance and the reflective and absorptive processes become dominant. The time for these phenomena to occur is approximately 25 nsecs after the start of the laser pulse.

The narrowing of the reflected laser pulse at power densities below plasma threshold is due to the large drop in the value of the reflection coefficient caused by thermal damage. Ignoring any scattering at other wavelengths, the 42% drop in reflection at power densities greater than $10^9 W/cm^2$ indicates that absorption in the plasma transition layer may be occurring. The 42% decrease is consistent with the findings of Basov *et al.*, and it yields an absorption coefficient of 0.545. Using Dawson's analysis, complementing it with the analysis of Lubin *et al.*, and inserting the value of the observed absorption coefficient, the density fall-off distance is on the order of 10^{-5}cm. This is consistent with the theory of Basov *et al.* that the length of the transition layer is on the order of the mean free path of a photon.

The narrowing and eventual disappearance of the reflected pulse may be due to the redirection of the scattered beam into

the vacuum chamber wall by the rapidly expanding plasma. However, analysis of the data by Brooks shows that only a critical density layer at the target surface and perpendicular to the incident beam could be responsible for redirecting the beam. Since Brooks' data was taken 10 nsecs after the plasma formation, only a crude extrapolation back to the target surface permitted this as a possibility.

The direction of the critical density gradient appears to be directed along the target normal in the early stages of the plasma formation. This was based upon the idea that the largest pressure gradient was along the specular direction and could not be parallel to the critical density gradient. It was assumed that the critical density gradient was associated with the largest pressure gradient.

By using the results of Shearer (Ref. 10) for oblique incidence, a critical density gradient normal to the target was consistent with the observed absorption coefficient and the resultant density fall-off distance. The direction of the critical density gradient is also compatible with the data indicating that most of the radiation was scattered in the specular direction.

VIII. RECOMMENDATIONS REGARDING FURTHER RESEARCH

When calculating the observed absorption coefficient, reflection at wave lengths other than 1.06 μ was ignored. In order to obtain a better estimate of the amount of incident energy deposited in the plasma, measurements should be taken to observe other frequencies. This could be done crudely through band pass filters or more precisely through spectral measurements.

The plasma density characteristics close to the target in the region of interest have been inferred from reflection and transmission measurements. However, measurements of currents in the target generated by the inhomogeneous blow-off of the electrons and ions could resolve the density characteristics in the region too close for an electric probe. Also, high-speed photography could be employed to obtain a better understanding of the plasma propagation in the direction of the laser beam.

Due to the availability of only one fast detector, comparison of the reflected and transmitted signals was done at slightly different power densities. Another detector with an optical delay line would allow simultaneous comparison of the two signals.

Additionally, all measurements were made to explain two-dimensional plasma characteristics. A three-dimensional analysis is required to fully understand the development of

the plasma and the corresponding reflection and absorption characteristics. This also could be accomplished by using high-speed photography, or electronic probes.

As far as the conclusions about the direction of the critical density gradient are concerned, more could be said if the plasma temperature, T_E, could be mapped the way Brooks mapped the density contours. Such contours may reveal the relative directions of the temperature and density gradients in the early plasma.

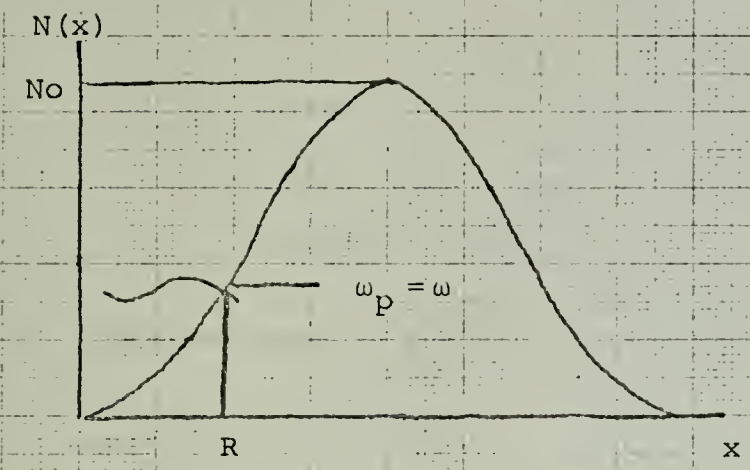

Fig. (1) Incident frequency matching the plasma frequency in the linear region of electron density profile.

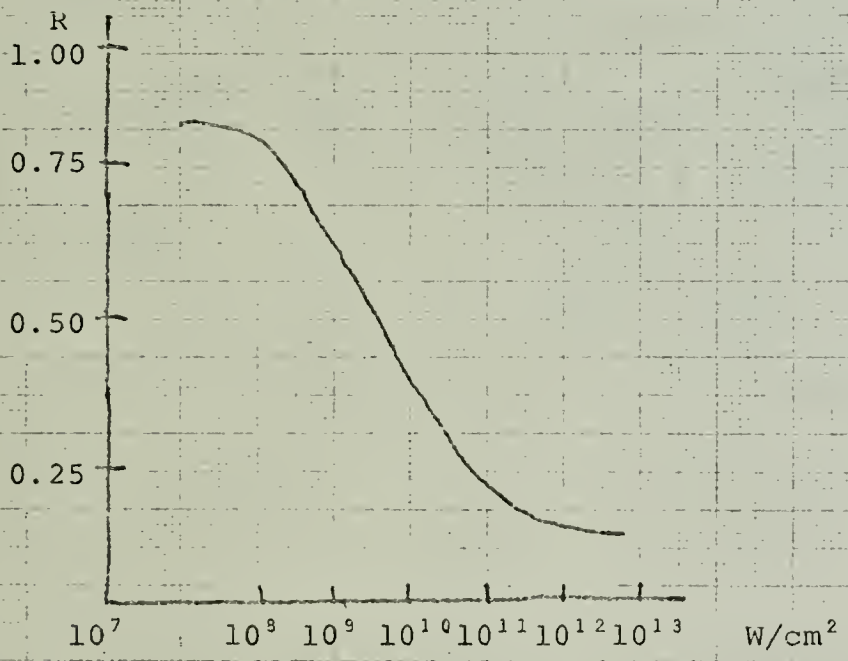

Fig. (2) Dependance of the Reflection coefficient on the flux density for aluminum (Basov, Ref. 11)

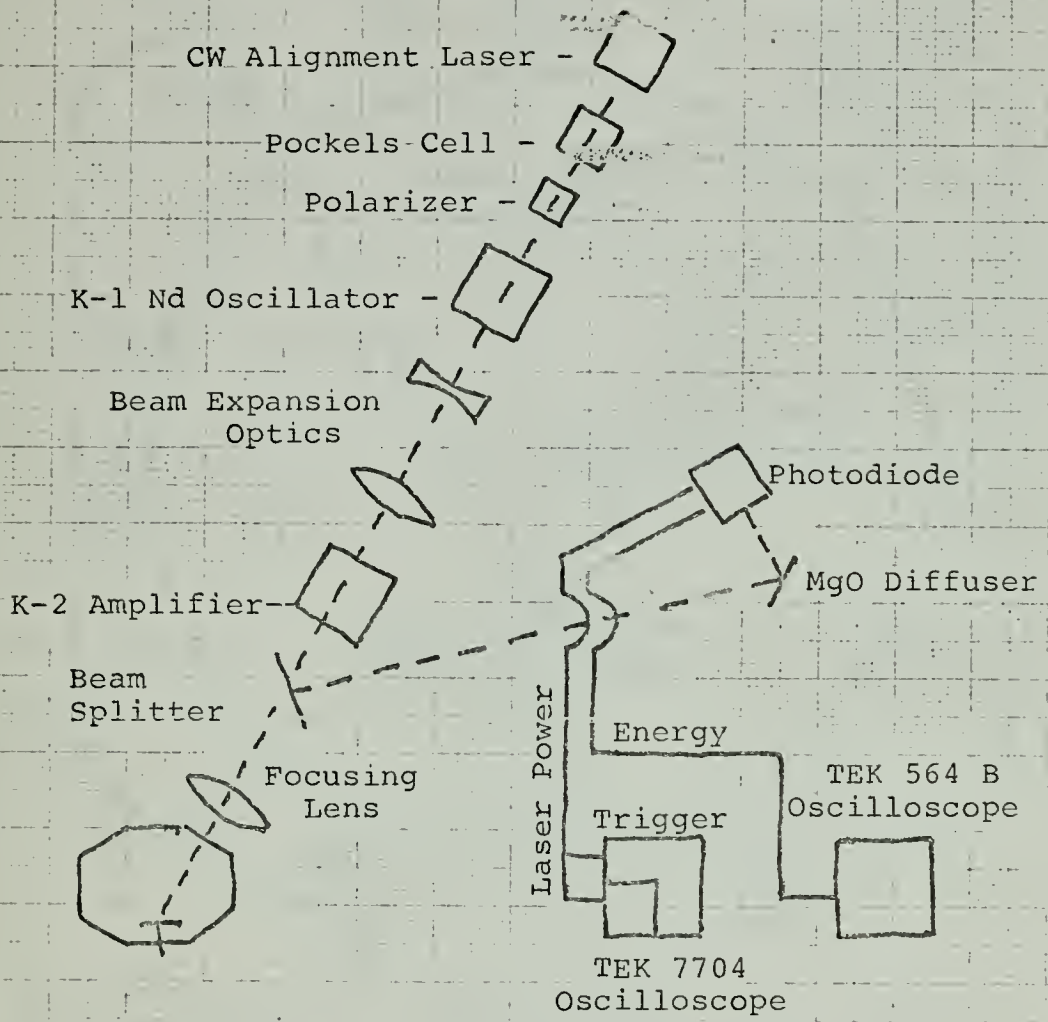

Fig. (3) Block Diagram of the General Experimental Layout.

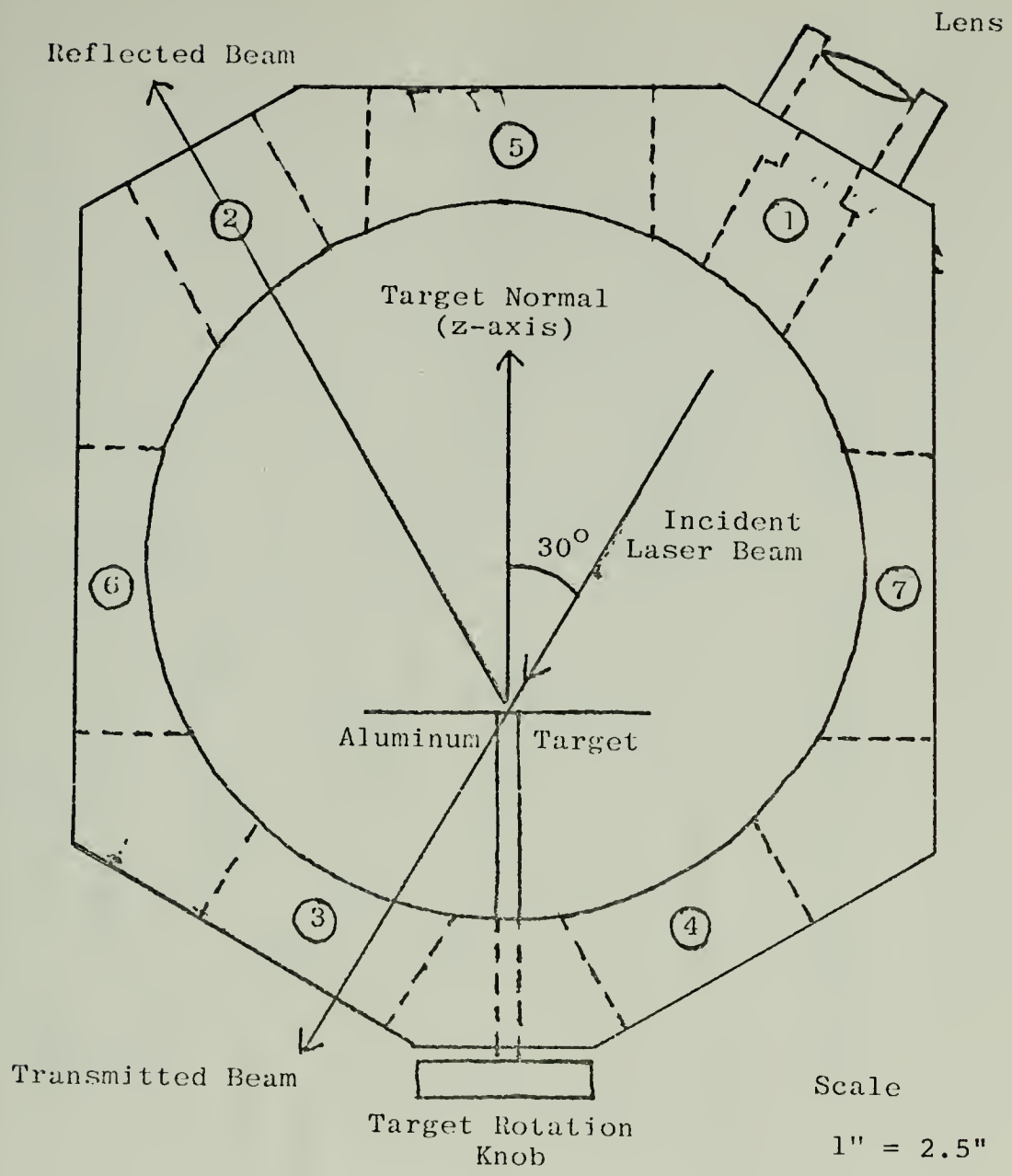

Figure 4. Top view of vacuum chamber.

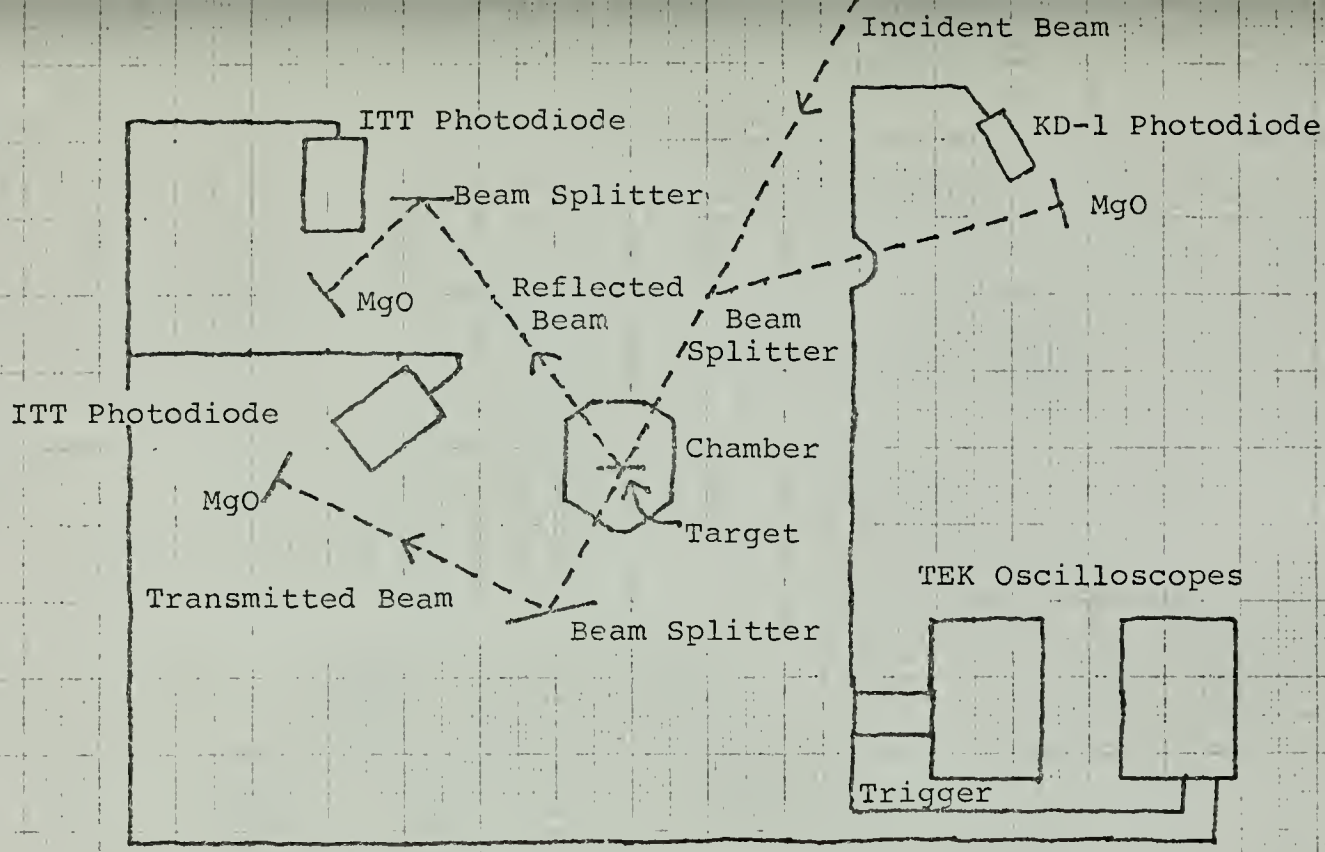

Fig. (5) Arrangement for making reflection and transmission measurements.

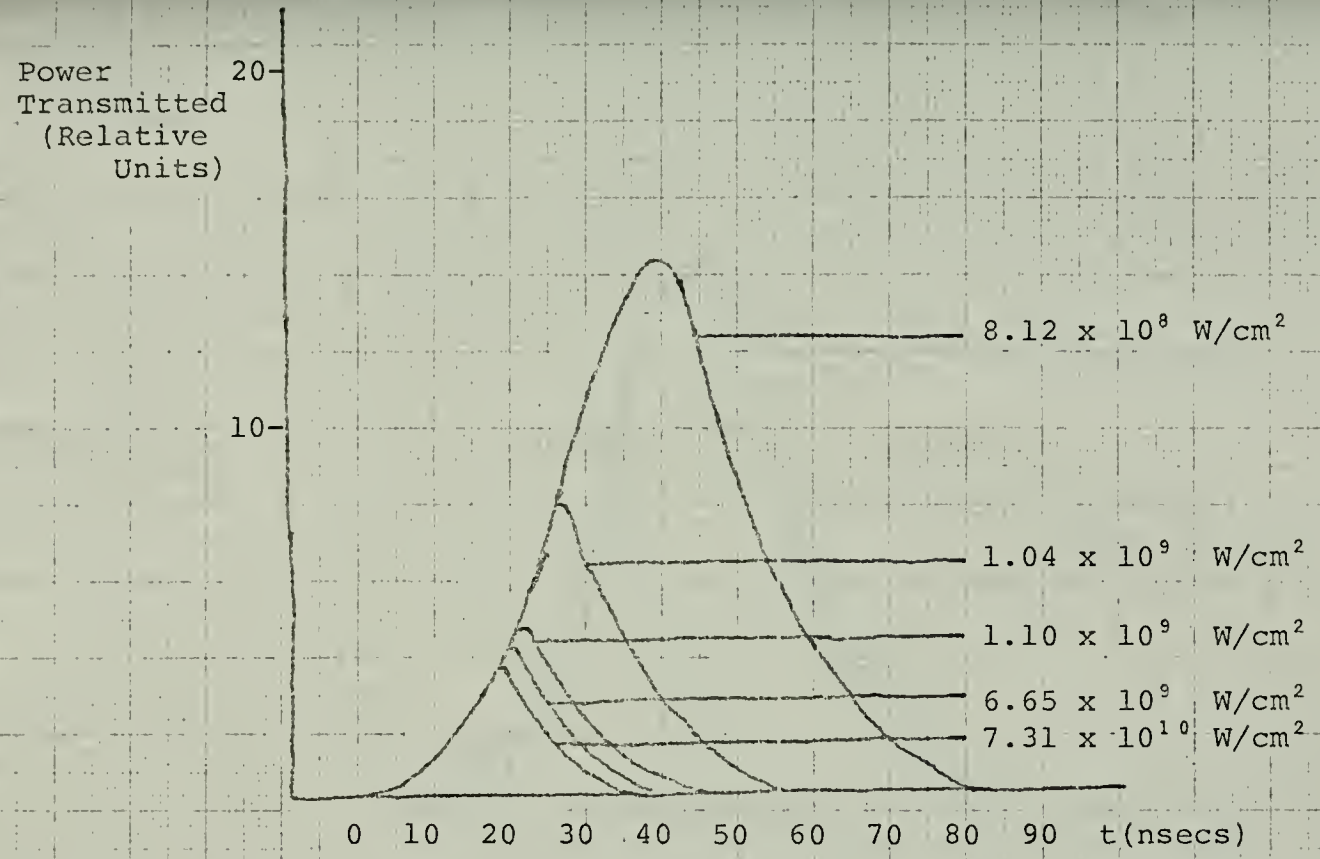

Fig. (6) Power transmitted vs time as a function of power density.

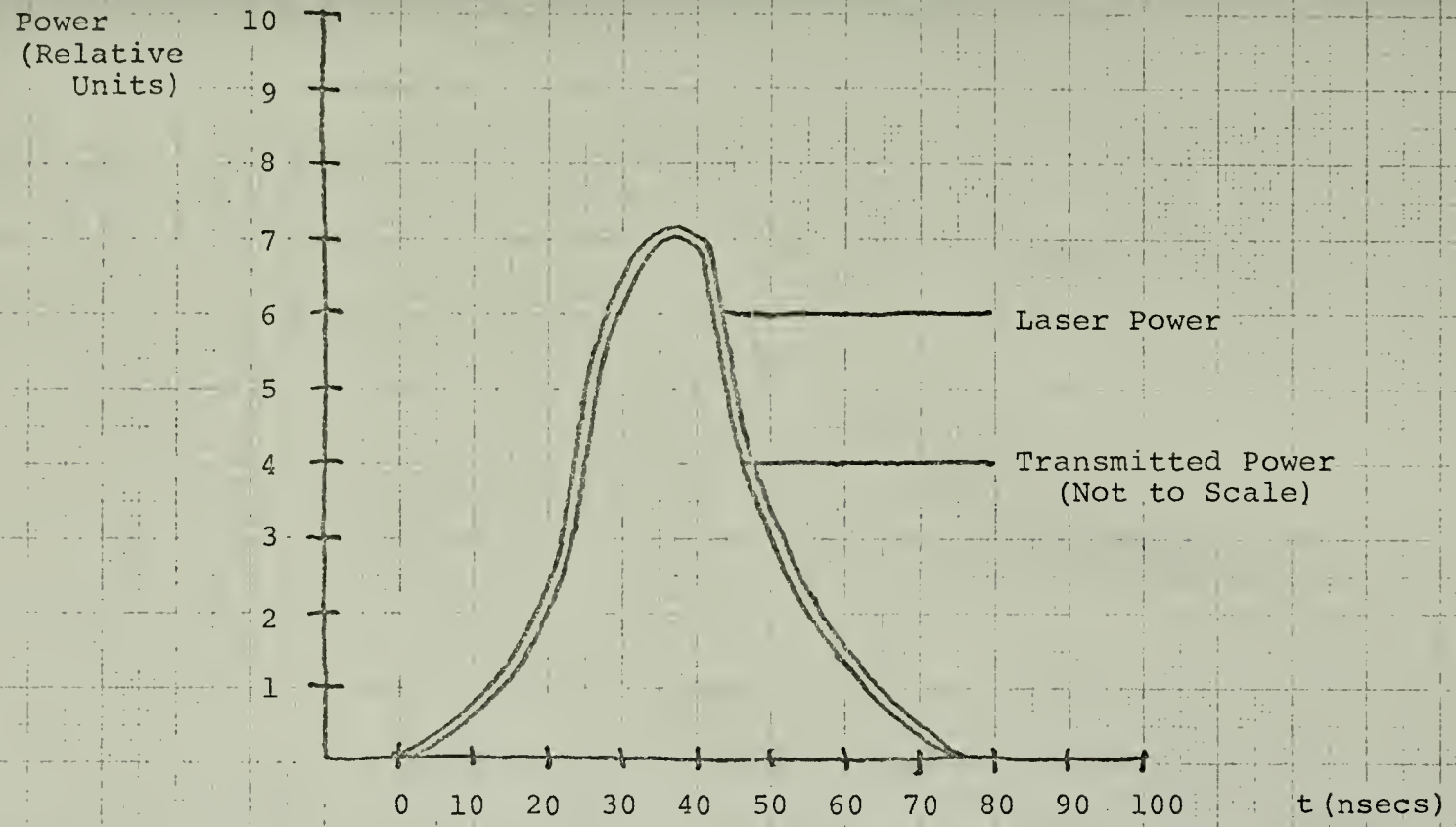

Fig. (7) Laser power and transmitted power vs time

For $P_D = 8.1 \times 10^8$ W/cm^2.

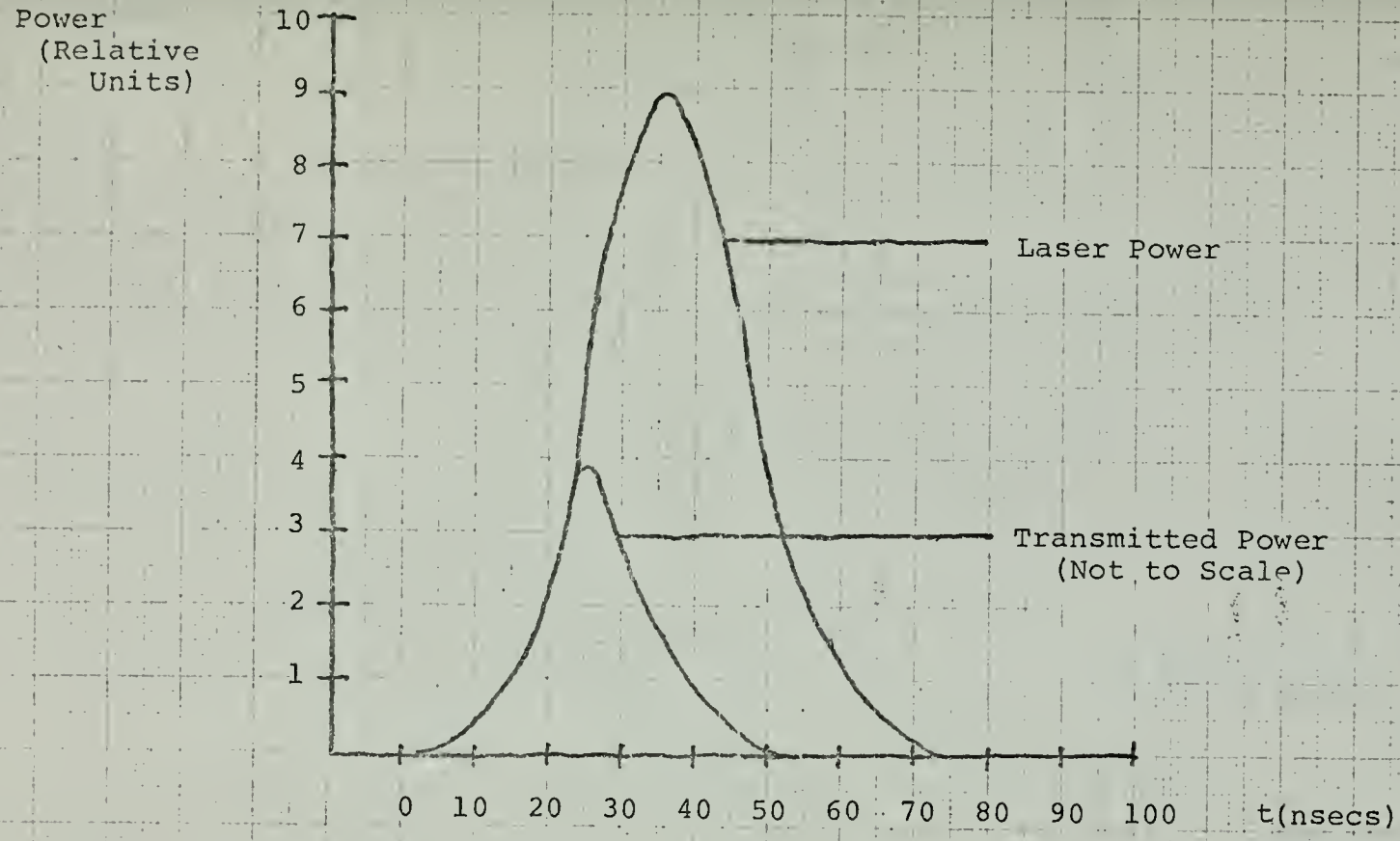

Fig. (8) Laser power and transmitted power vs time

For $P_D = 1.1 \times 10^9$ W/cm^2.

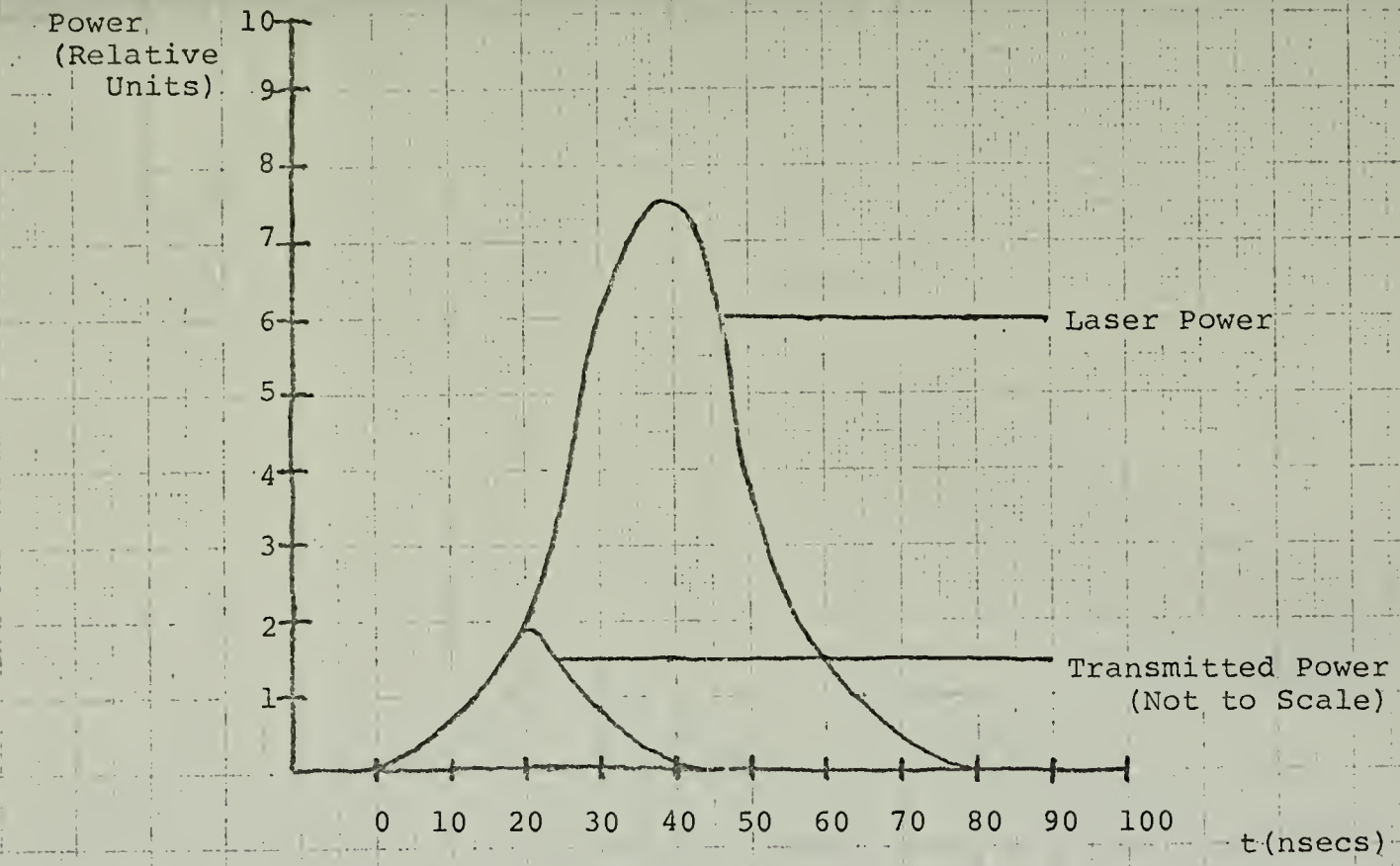

Fig. (9) Laser power and transmitted power vs time

For $P_D = 1.5 \times 10^9$ W/cm^2.

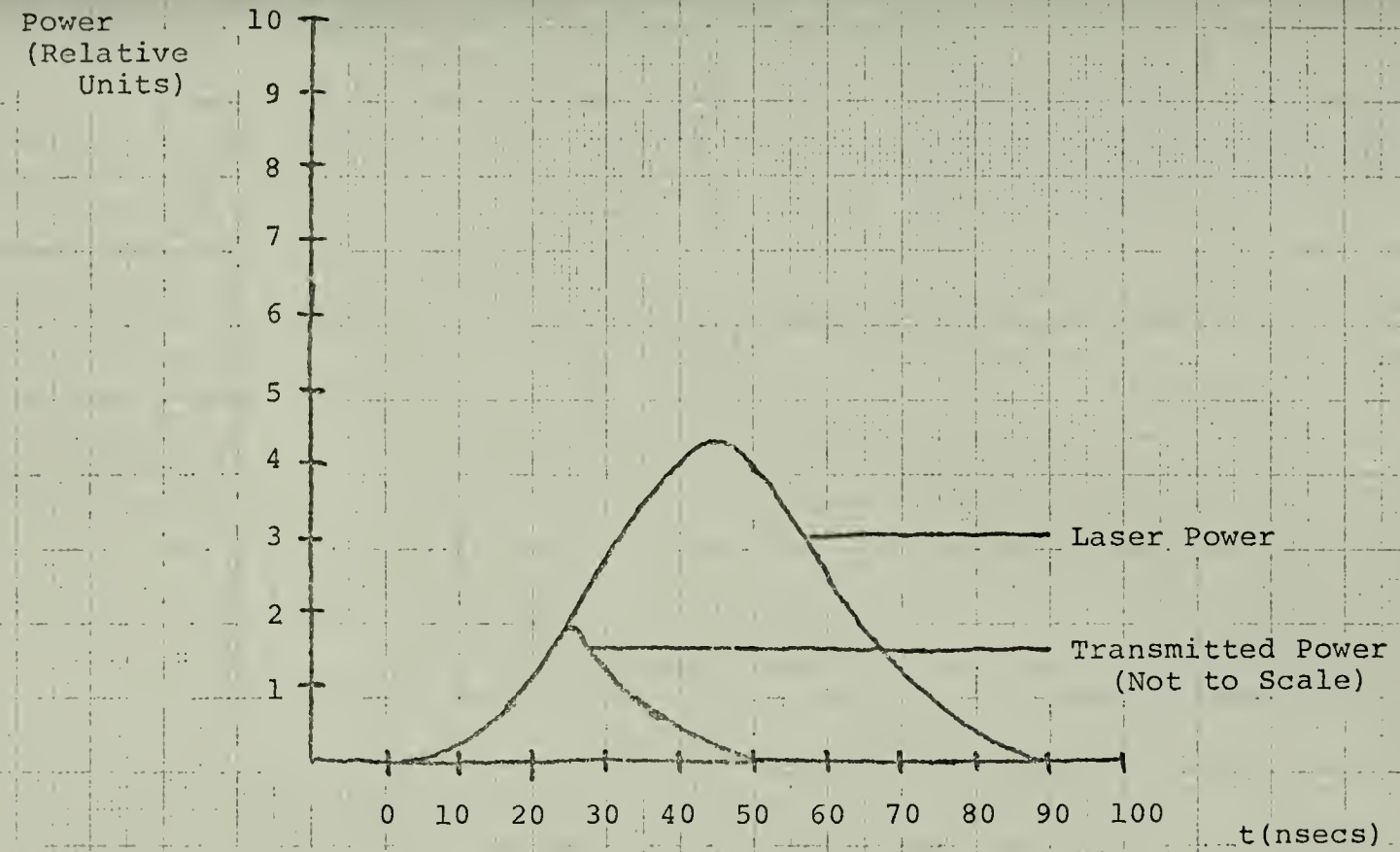

Fig. (10) Laser power and transmitted power vs time

For $P_D = 4.1 \times 10^9$ W/cm^2.

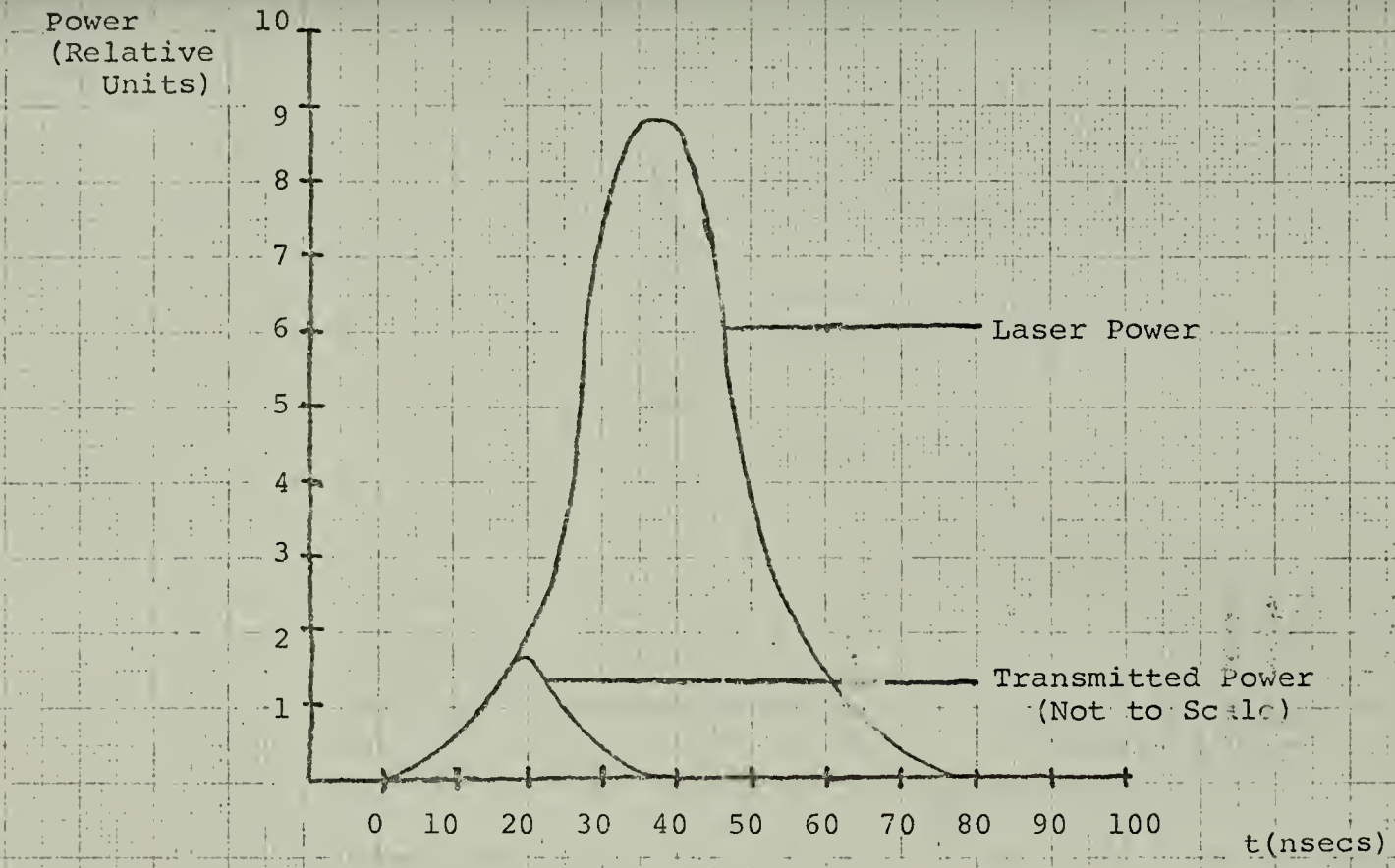

Fig. (11) Laser power and transmitted power vs time

For $P_D = 6.7 \times 10^3$ W/cm^2.

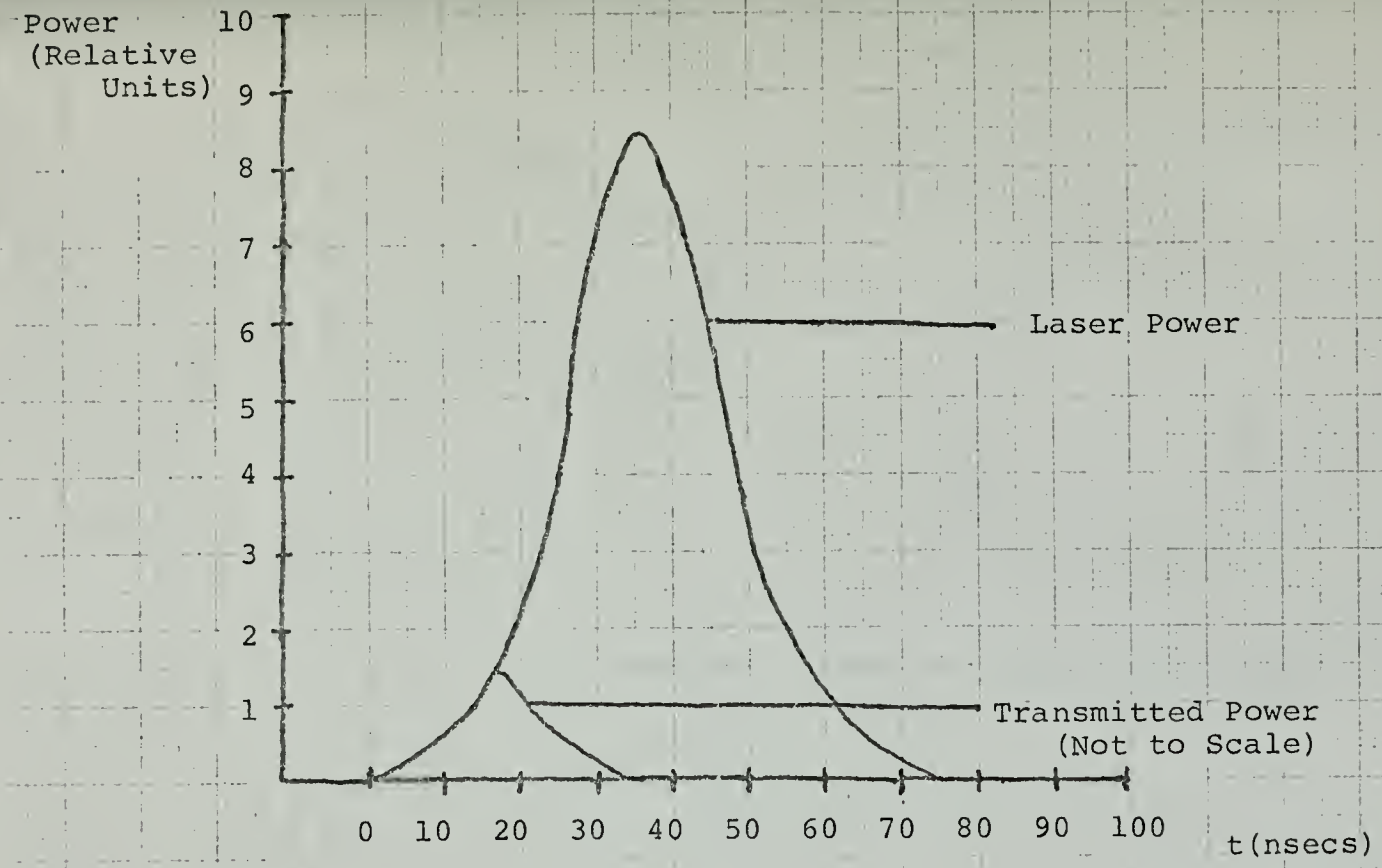

Fig. (12) Laser power and transmitted power vs time

For $P_D = 7.3 \times 10^{10}$ W/cm^2.

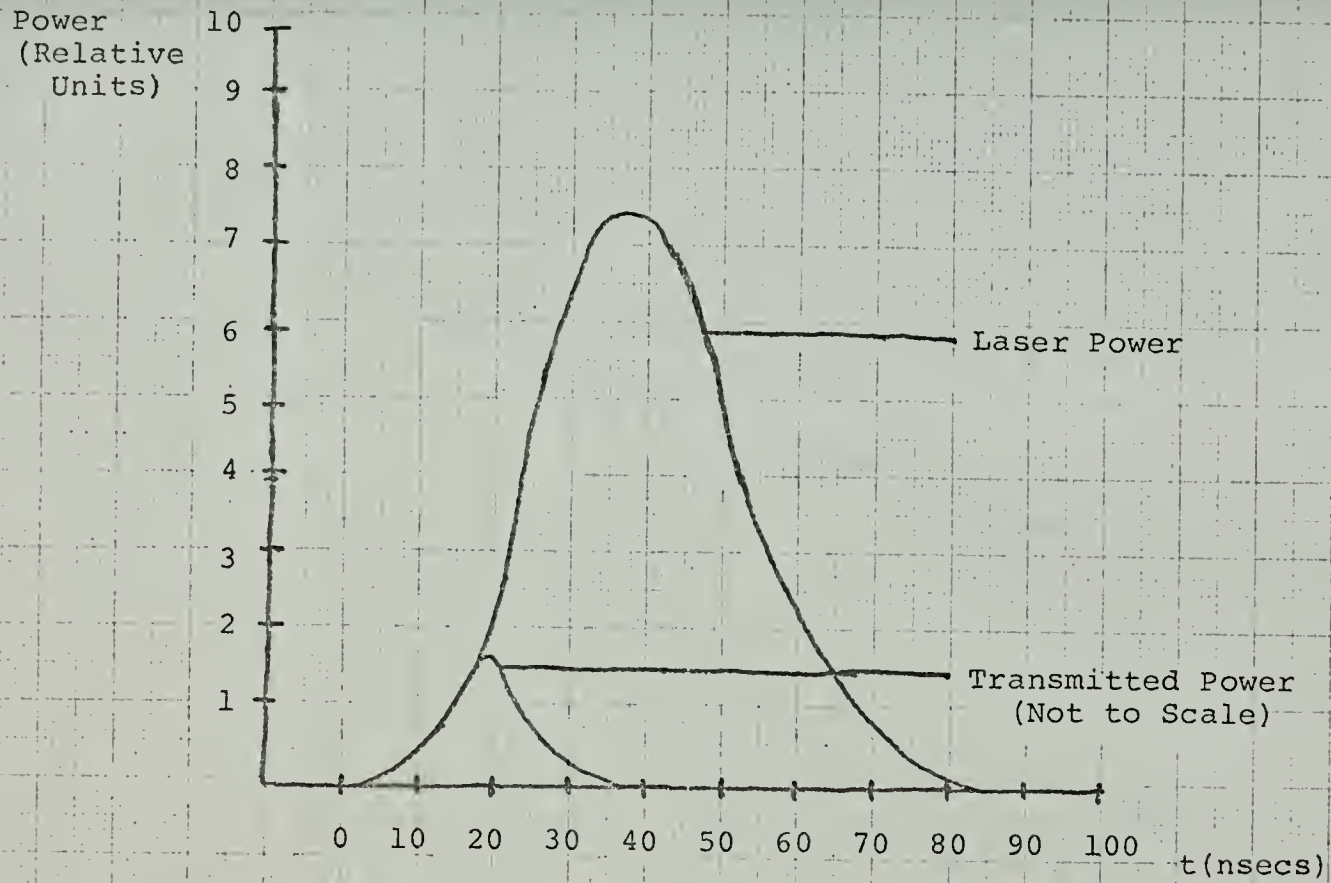

Fig. (13) Laser power and transmitted power vs time

For $P_D = 8.0 \times 10^{10}$ W/cm^2.

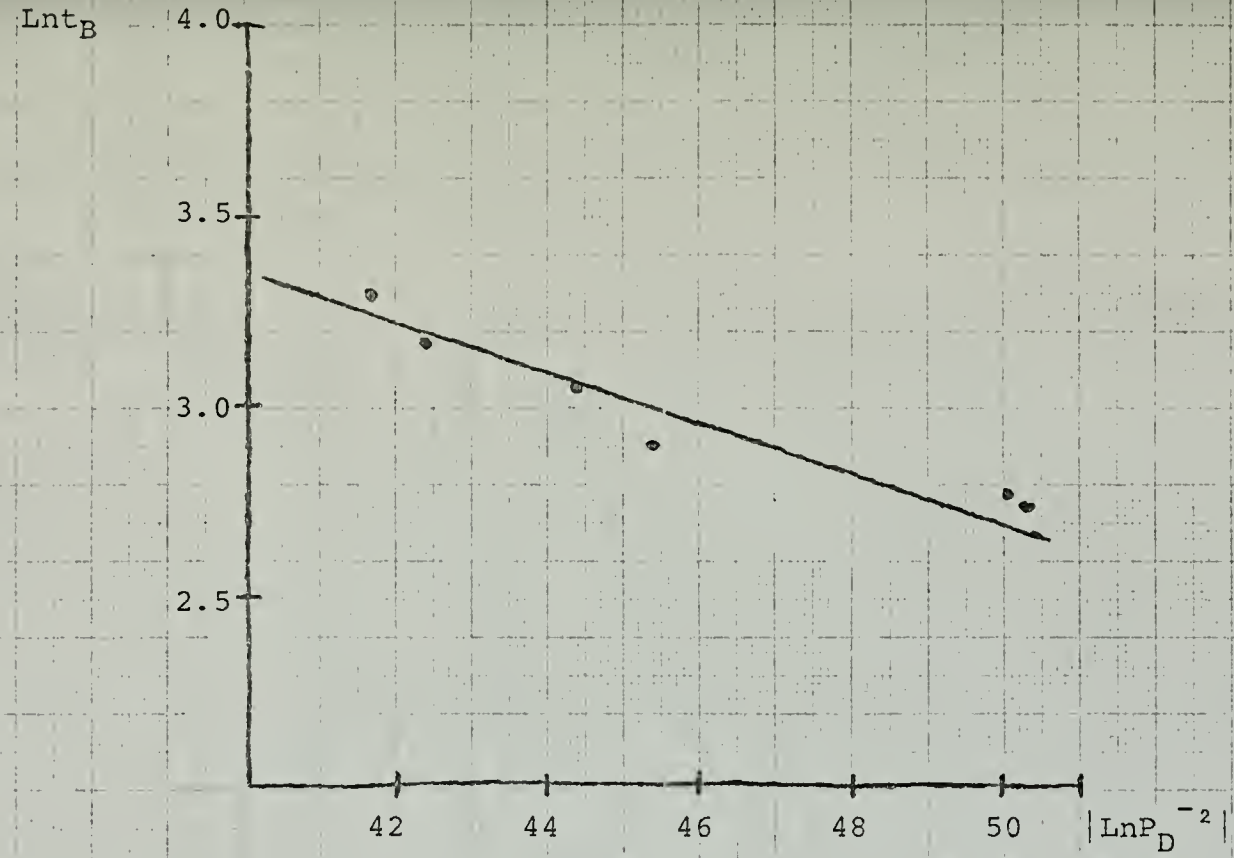

Fig. (14) Lnt_C vs $|LnP_D^{-2}|$

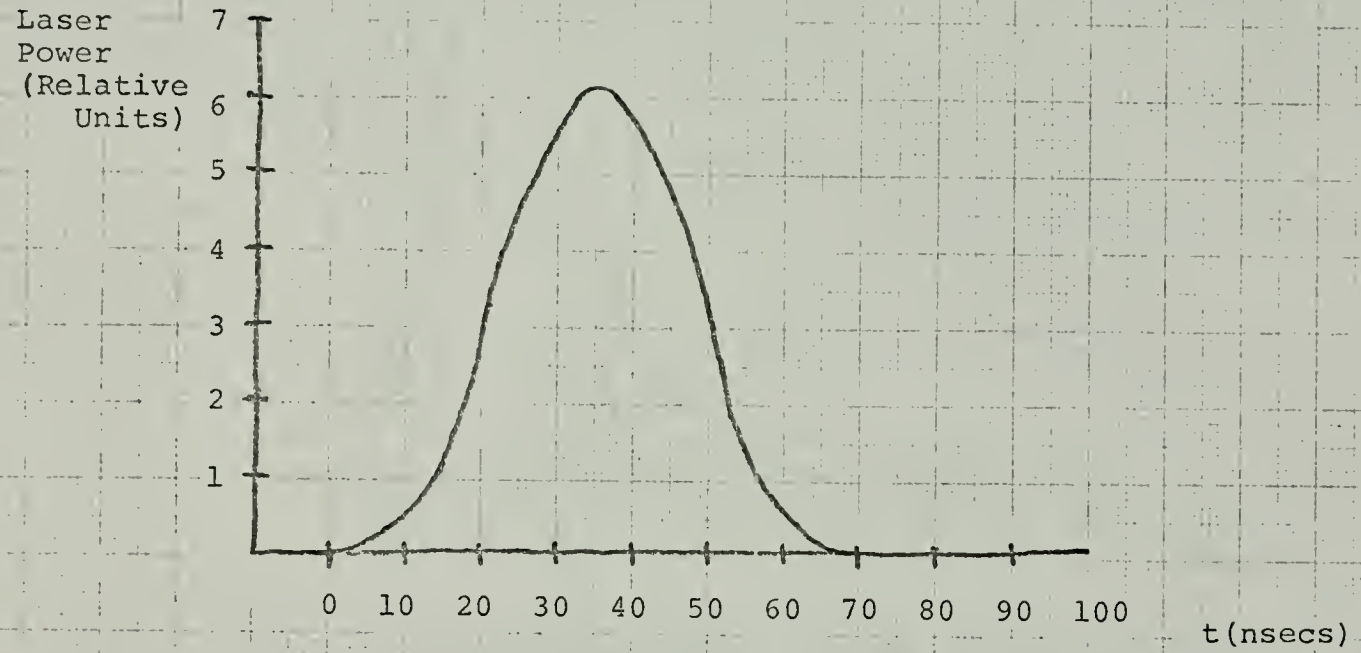

Fig. (15) Representative laser power pulse during reflection measurements.

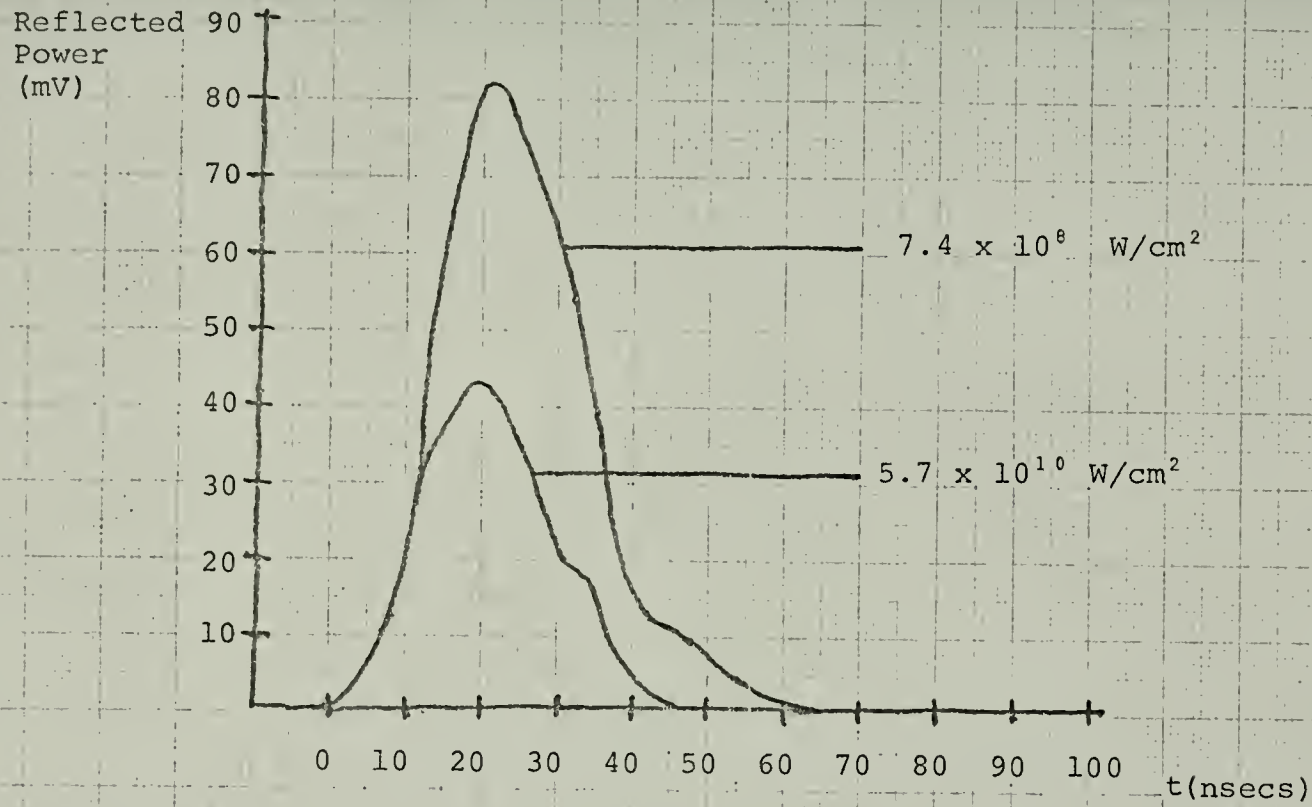

Fig. (16) Reflected power vs time for power densities below and above plasma threshold in specular direction.

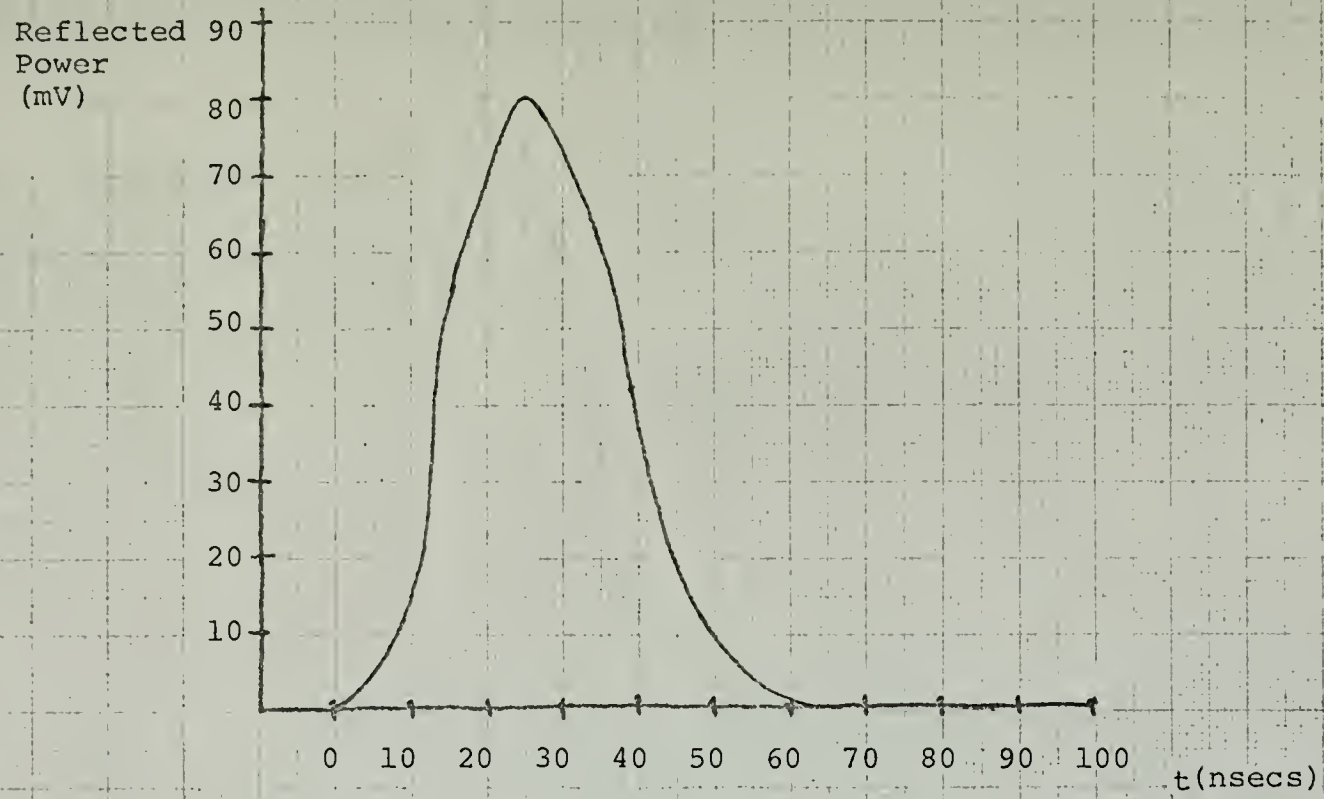

Fig. (17) Reflection signal vs time

For $P_D = 6.6 \times 10^8$ W/cm^2 in specular direction.

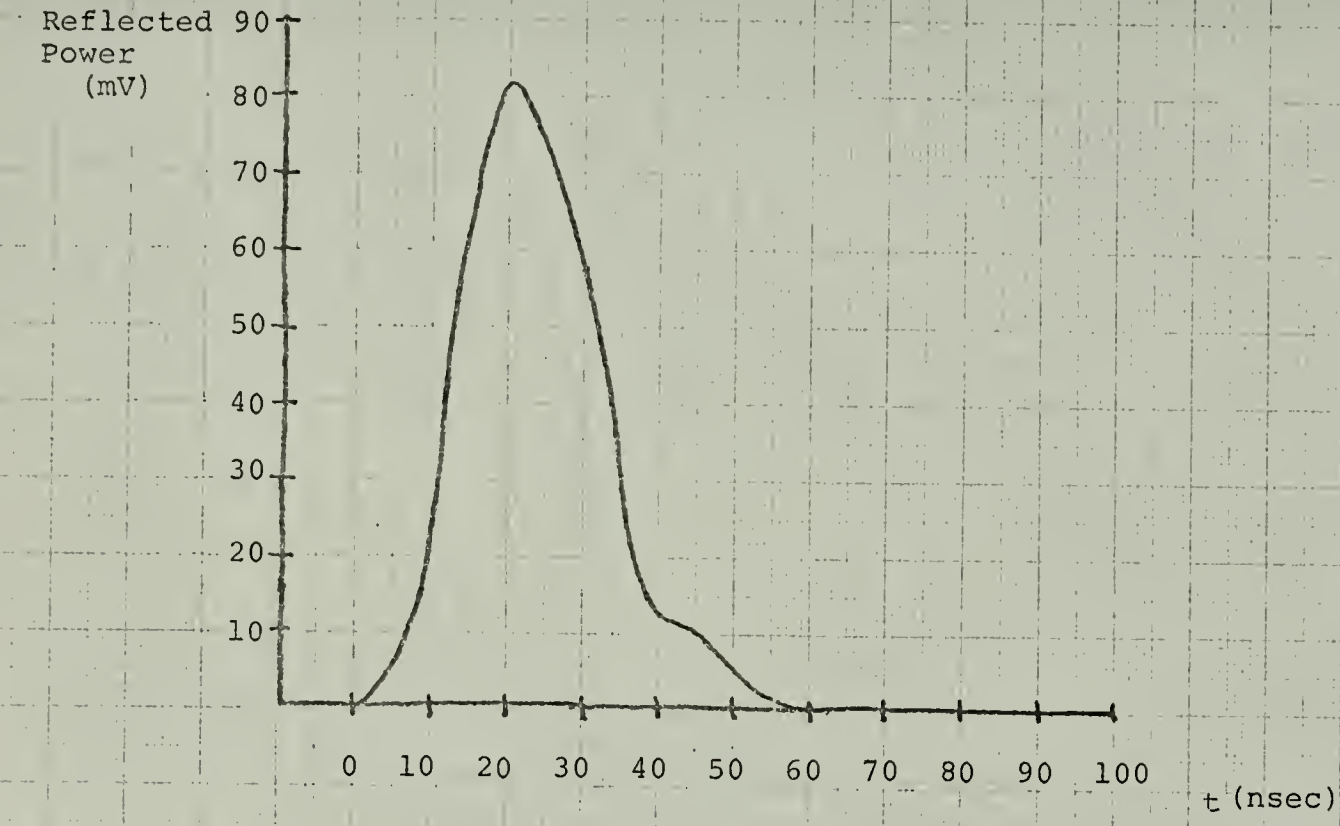

Fig. (18) Reflected power vs time (nsecs)

For $P_D = 7.4 \times 10^8$ W/cm^2 in specular direction.

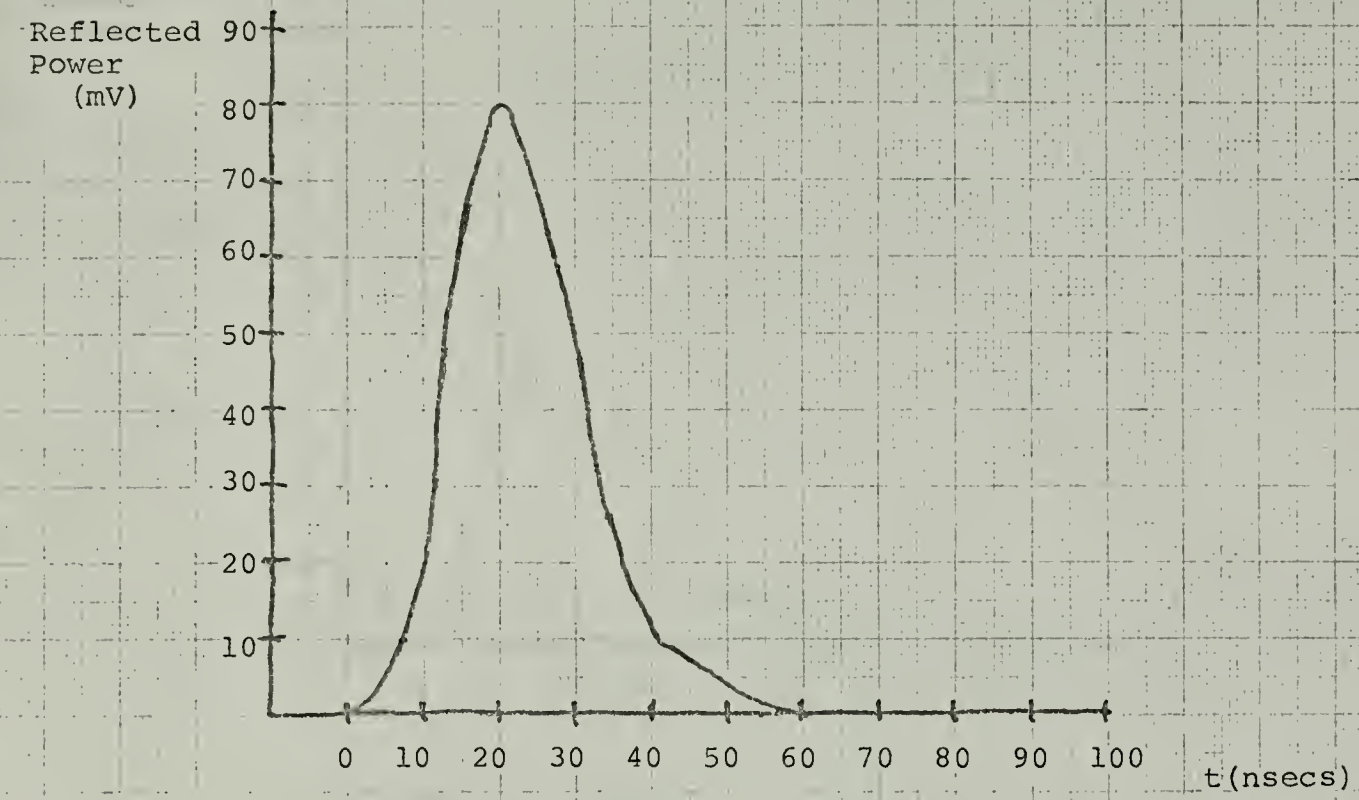

Fig. (19) Reflected power vs time (nsecs) at $P_D = 7.1 \times 10^8$ W/cm^2 in specular direction.

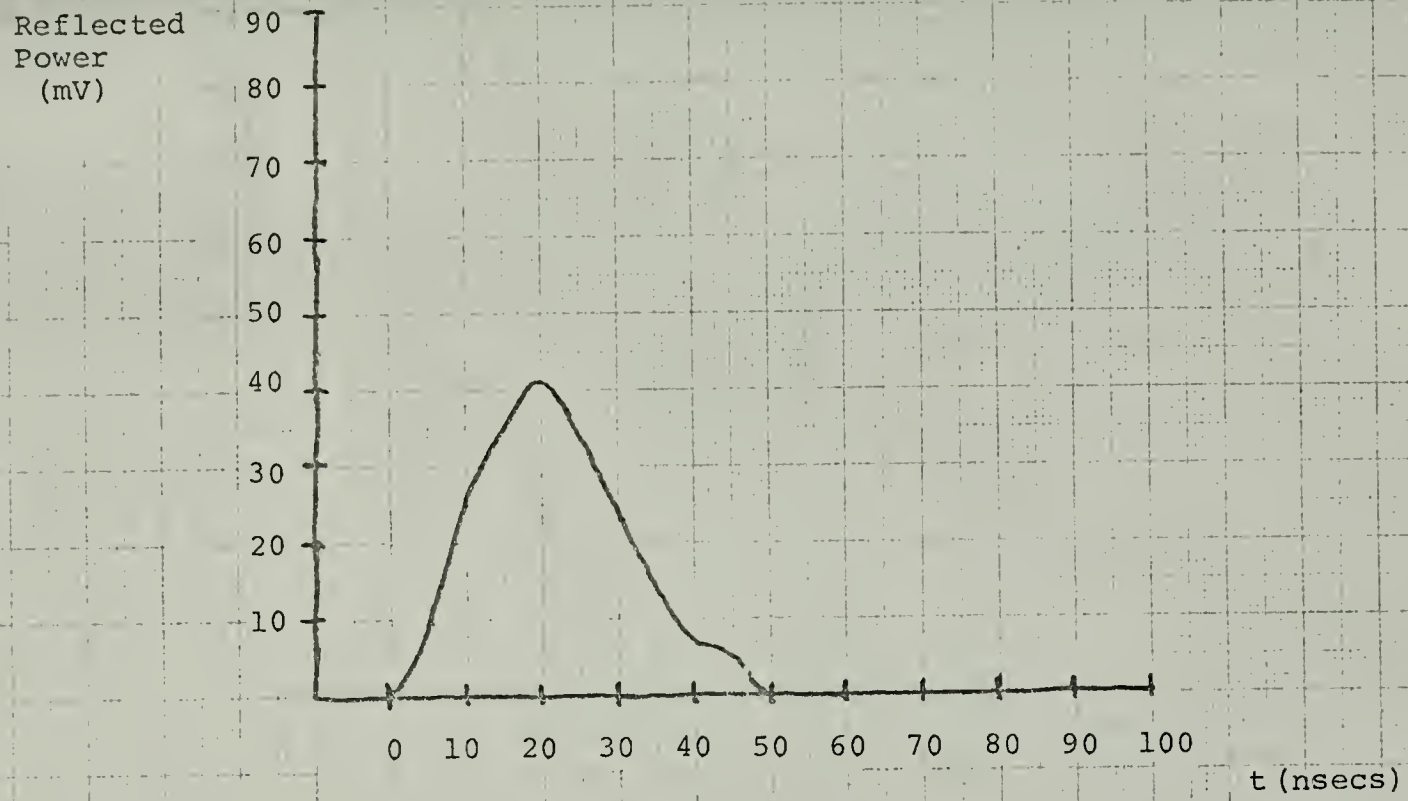

Fig. (20) Reflected power vs time (nsecs)

For $P_D = 3.8 \times 10^9$ W/cm^2 in specular direction.

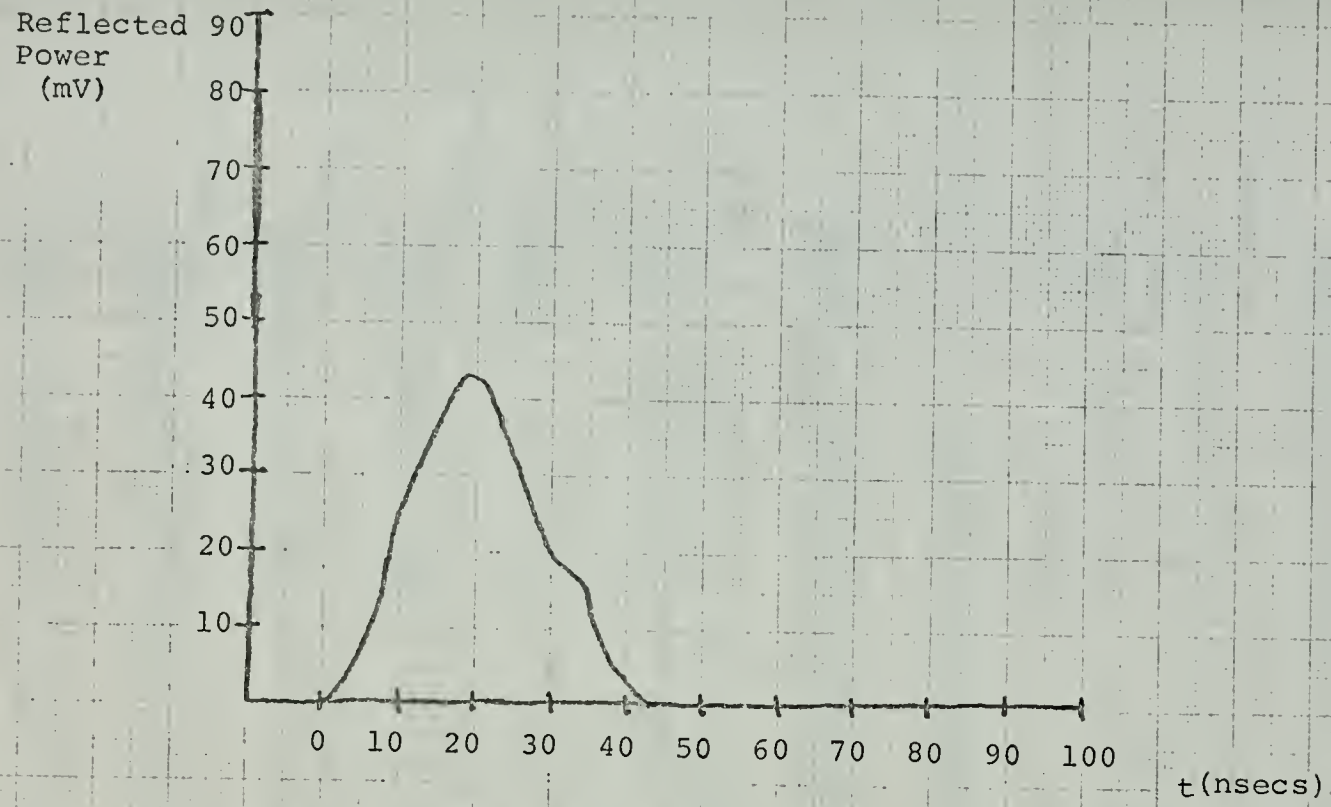

Fig. (21) Reflected power vs time (nsecs)

For $P_D = 5.7 \times 10^{10}$ W/cm^2 in specular direction.

BIBLIOGRAPHY

1. Basov, N. G. and Krokhin, O. N., Condition for Heating Up of a Plasma by the Radiation from an Optical Generator, Soviet Physics-JETP 19, 123, 1964.

2. Dawson, J. M., On the Production of Plasmas by Giant Pluse Lasers, Phys. Fluids 7, 981, 1964.

3. Hertzberg, A., Daiber, J. W., and Witliff, C. E., Laser Generated Implosions, Phys. Fluids 9, 617, 1966.

4. Breuckner, K. A. and Jorna, S., Laser Driven Fusion, Rev. Mod. Phys., Vol. 46, No. 2, April, 1974.

5. Ready, J. F., Effects of High Power Laser Radiation, Academic Press, New York, 1971.

6. Brooks, K. M., An Investigation of Early Disturbances Found in Association with Laser Produced Plasmas, M.S. Thesis, Naval Postgraduate School, 1973.

7. Smith, D. C. and Fowler, M. C., Ignition and Maintenance of CW Plasma in Air with CO_2 Laser Radiation, invited paper annual meeting of Optical Society of America, 1974.

8. Dawson, J. M., "Radiation from Plasma," Advances in Plasma Physics, Vol. 1, Wiley, 1968.

9. Dawson, J. M., Kaw, P., and Green, B., Optical Absorption and Expansion of Laser Produced Plasmas, Phys. Fluids, Vol. 12, No. 4, 1969.

10. Shearer, J. W., Effect of Oblique Incidence of Optical Absorption of Laser Light by a Plasma, Phys. Fluids, Vol. 14, No. 1, 1971.

11. Basov et al., Reduction of Reflection Coefficient for Intense Laser Radiation on Solid Surfaces, Sov. Phys.-Tech. Phys., JETP, Vol. 13, No. 1, 1969.

12. Davis, L. J., Self-Generated Magnetic Fields Produced by Laser Bombardment of a Solid Target, M.S. Thesis, Naval Postgraduate School, 1971.

13. Bystrova, T. B., et al., Multiphoton Ionization of Xenon and Krypton Atoms at Wavelength $\lambda = 1.06\ \mu$, Sov. Phys.-Tech. Phys., JETP Lett. 5, 178, 1967.

14. Voronov, G. S., et al., Multiphoton Ionization of Hydrogen Molecule in the Strong Electric Field of Ruby Laser Emission, Sov. Phys. - Tech. Phys., JETP Lett. 2, 237, 1965.

15. Delone, G. A., et al., Role of the Field Intensity and Structure of the Atom in the Process of Multiphoton Ionization, Sov. Phys. - Tech. Phys., JETP Lett. 9, 59, 1969.

16. Lubin et al., "Laser Heated Overdense Plasmas," Laser Interaction and Related Plasma Phenomenon, Vol. 2, Plenum Press, Schwarz and Hora, Eds., 1972.

17. Wegener, B., Measurements of Early Magnetic Fields in Laser Produced Plasmas, M.S. Thesis, Naval Post-graduate School, 1974.

18. Schwirzke, F., Measurements of Spontaneous Magnetic Fields in Laser Produced Plasmas, invited paper, Third Workshop on "Laser Interaction and Related Plasma Phenomenon," 1973.

19. Handbook of Physics and Chemistry, Chemical Rubber Company, 1971-1972.

20. Lee, P., Giovanielli, D. V., and Godwin, R. P., Harmonic Generation and Frequency Mixing in Laser-Produced Plasmas, App. Phys. Letts., Vol 24, No. 9, 1974.

21. Ozizmir, E., Transmission and Reflection of Electromagnetic Waves at the Boundary of a Relativistic Collisionless Plasma, Journal of Math. Phys., Vol. 9, No. 13, 1974.

22. Tanaka, K. and Hazama, K., Reflection and Transmission of Electromagnetic Waves by a Moving Inhomogeneous Medium, Radio Science, Vol. 7, No. 10, 1972.

23. Clemmow, P. C. and Karunarathne, V. B., Reflexion of a Plane Wave at a Plasma Half Space, Journal of Plasma Phys., Vol. 4, Part 1, 67, 1970.

24. Stamper, J. A., et al., Spontaneous Magnetic Fields in Laser-Produced Plasmas, Phys. Rev. Letts., Vol. 26, No. 17, 1971.

25. Shohet, J. L., The Plasma State, Academic Press, 1971.

26. Fowles, G. R., Introduction to Modern Optics, Holt, Rhinehart and Winston, Inc., 1968.

27. Spitzer, L., Physics of Fully Ionized Gases, 2nd Ed., Wiley, 1962.

28. Tannenbaum, B. S., Plasma Physics, McGraw-Hill, 1967.

29. Schriempf, J. T., Effects of High Energy Laser Radiation: A Short Course, Naval Postgraduate School. NRL Report 7728, 1974.

INITIAL DISTRIBUTION LIST

		No. Copies
1.	Defense Documentation Center Cameron Station Alexandria, Virginia 22314	2
2.	Library, Code 0212 Naval Postgraduate School Monterey, California 93940	2
3.	Department Chairman, Code 61 Wh Department of Physics and Chemistry Naval Postgraduate School Monterey, California 93940	2
4.	Professor A. W. Cooper, Code 61 Cr Department of Physics and Chemistry Naval Postgraduate School Monterey, California 93940	5
5.	LCDR Thomas H. Butler CINCPACFLT 1200 PSI Propulsion Examining Board Box 70 San Diego, California 92136	1

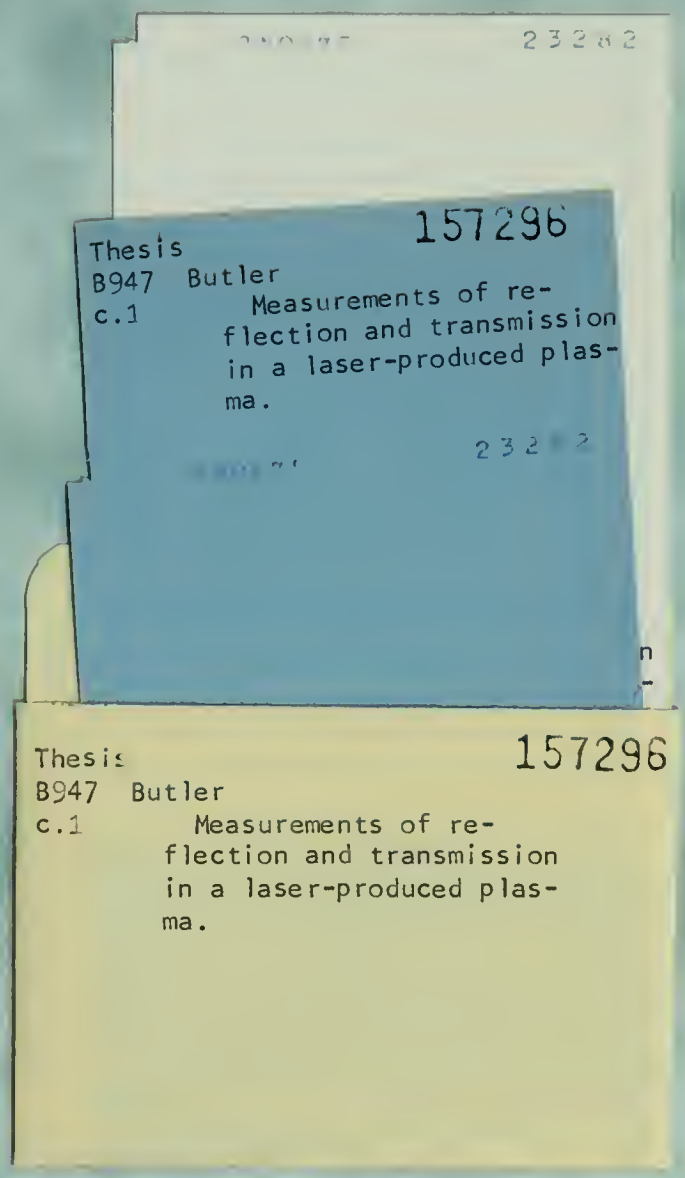
157296
Thesis
B947 Butler
c.1 Measurements of re-
flection and transmission
in a laser-produced plas-
ma.

thesB947
Measurements of reflection and transmiss
3 2768 002 08856 9
DUDLEY KNOX LIBRARY